

国土技術政策総合研究所資料

TECHNICAL NOTE of
National Institute for Land and Infrastructure Management

No.1110

April 2020

Guideline for the interpretation of sediment-related disasters by synthetic aperture radar (SAR) images

SUZUKI Yamato
MATSUDA Masayuki
TAKIGUCHI Shigetaka
NOMURA Yasuhiro
YAMASHITA Kumiko
NAKAYA Hiroaki

国土交通省 国土技術政策総合研究所

National Institute for Land and Infrastructure Management
Ministry of Land, Infrastructure, Transport and Tourism, Japan

Guideline for the interpretation of sediment-related disasters by synthetic aperture radar (SAR) images

SUZUKI Yamato*, MATSUDA Masayuki**, TAKIGUCHI Shigetaka***,
NOMURA Yasuhiro ****, YAMASHITA Kumiko*****, NAKAYA Hiroaki*****

Synopsis

This guideline describes synthetic aperture radar images interpretation of sediment-related disasters that can be used even at night or under adverse weather conditions, in order to enable to identify disaster-stricken area.

Key Words: SAR Image, Slope Collapse, Sediment-related Disaster, Landslide Dam,
Image Interpretation, Backscatter Coefficient

*	土砂災害研究室研究官	Researcher, Sabo Risk-Management Division
**	土砂災害研究室交流研究員	Guest Research Engineer, Sabo Risk-Management Division
***	土砂災害研究室主任研究官	Senior Researcher, Sabo Risk-Management Division
****	前土砂災害研究室主任研究官	Former Senior Researcher, Sabo Risk-Management Division
*****	前土砂災害研究室交流研究員	Former Guest Research Engineer, Sabo Risk-Management Division
*****	土砂災害研究室長	Head, Sabo Risk-Management Division

[Introduction]

When Sediment deposition occurs in a channel as a result of occurrence of a large-scale slope failure or deep failure, an inundated area may be formed by the damming up of the river. The sediment that has blocked the channel is often unstable, and if the inundated area has expanded rapidly, a dam failure or the like may occur, thereby causing serious damage to the lower reaches, and therefore a quick grasping of the situation after the disaster is required. In addition, it is also important to grasp the place where the slope failure or deep failure occurred in a concentrated manner as well as the range of such occurrence, similarly, in order to contribute to early commencement of first-aid measures.

The National Institute for Land and Infrastructure Management has been engaging heretofore in a study of techniques for quickly grasping the location of channel blockage, by focusing on reading by using images of Synthetic Aperture Radar (hereinafter called "SAR") that enables observation to be made day and night in any weather condition. The results of such study were summarized as Technical Note of National Institute for Land and Infrastructure Management No. 760 of November 2013 "Method of emergency search for the location of landslide dams using high-resolution single-polarization SAR image interpretation" (hereinafter called "NILIM Technical Note No. 760"). After that, it was developed into an extraction technique using high-resolution dual-polarized SAR images, in order to grasp the location of channel blockage more quickly and reliably, and the results of such development were summarized as Technical Note of National Institute for Land and Infrastructure Management No. 791 of June 2014 "Method of emergency search for the location of landslide dams and collapses using high-resolution dual-polarization SAR image interpretation" (hereinafter called "NILIM Technical Note No. 791").

In recent years, opportunities are increasing in which SAR images before and after a disaster can be utilized by making use of data that are continually accumulated by steady state observation. NILIM has devised a method for utilizing its findings heretofore and at the same time for engaging in image interpretation survey of a sediment disaster by using SAR images before and after the disaster, and has applied the method to response to the disasters in recent years. Consequently, it has been clarified that the method can extract not only large-scale slope failures that have been researched until the present, but also smaller failure phenomena as well as locations where the topography and land cover have undergone changes, and that the situation of damage can be grasped in a short period of time regarding the sediment disasters where slope failures occur in a wide range and with a high density as well. This material explains the method for the interpretation of sediment disasters by means of SAR images, and at the same time has summarized the conditions of

application and the precautions. Now that further utilization of satellite images, etc. is required in order to improve the efficiency of the Regional Development Bureaus, etc. during response to disasters, it is our hope that this material will serve as a reference, as one of the techniques for supporting an appropriate initial investigation by narrowing down the range of damage at an early stage.

This material is part of the results of a joint research with the Japan Aerospace Exploration Agency, a National Research and Development Agency, (hereinafter called the "JAXA"), i.e. the "Joint research on the development of methods to monitor landslide/mudflow using Daichi 2, the advanced land observing satellite" (FY 2017-).

April 2020 Sediment Disaster Risk Management Division, Sediment Disaster Research Department,

NILIM

[Purpose and composition of this material]

This material shows the procedures and technical guidelines for the image interpretation survey of sediment disasters using SAR images to be carried out by the staff of a Regional Development Bureau and others at the time of occurrence of a sediment disaster. Also, since the material explains the basics and technical precautions concerning SAR images, we believe that the material can be utilized not only by persons in charge of disaster preparedness but by other technical personnel involved in the image interpretation survey of sediment disasters, etc. as well.

This material consists of the following 3 parts. See the Table of Contents for details.

Part 1 Basics concerning Synthetic Aperture Radar (SAR) images

It explains basics such as observation by means of SAR and the features of SAR images as well as precautions for use.

Part 2 Explanation of the techniques for the image interpretation survey of sediment disasters by means of SAR images

It explains the procedures for the interpretation of sediment disasters using SAR images.

Part 3 Results of application of the image interpretation survey of sediment disasters by means of intensity difference SAR images

It shows the results of application of the image interpretation survey of sediment disasters using intensity difference SAR images to actual disasters.

By utilizing this material together with the "Guide Book for Artificial Satellite Utilization during Disasters - Sediment Disaster Edition" (JAXA Satellite Applications and Operations Center, and Sabo (Erosion and Sediment Control) Planning Division, Sabo (Erosion and Sediment Control) Department, Water and Disaster Management Bureau, Ministry of Land, Infrastructure, Transport and Tourism), it is expected that the image interpretation survey of sediment disasters by means of more effective SAR images will be realized.

Guide for the Image Interpretation of Sediment Disasters by Using Synthetic
Aperture Radar (SAR) images

Table of Contents

Part 1 Basics concerning Synthetic Aperture Radar (SAR) images	1
1. Synthetic Aperture Radar (SAR)	1
1.1 Principles of SAR observation	1
1.2 Features of SAR	3
1.3 Wavelength (band)	5
1.4 Scattering characteristics	6
1.5 Polarization characteristics	9
2. SAR images	10
2.1 Generation of SAR images	10
2.2 Features of SAR images	12
2.3 Precautions for SAR images	13
2.4 Resolution of SAR images	16
2.5 Analysis and types of SAR images	17
3. Utilization of SAR images in the image interpretation survey of sediment disasters	20
3.1 Conditions of observation of SAR images suitable for the image interpretation survey of sediment disasters	20
3.2 Precautions when utilizing SAR images in the image interpretation survey of sediment disasters	21

Part 2 Explanations of the techniques for the image interpretation survey of sediment disasters by means of SAR images	24
1. Selection of the techniques for the image interpretation survey of sediment disasters by means of SAR images.....	24
1.1 Selection according to the conditions of available SAR images.....	24
1.2 Selection according to the scale of a sediment disaster to which the image interpretation survey is applicable	26
2. Image interpretation survey of sediment disasters by means of dual-polarized SAR images.....	27
3. Image interpretation survey of sediment disasters by means of intensity difference SAR images.....	28
3.1 Generation of intensity difference SAR images.....	28
3.2 Interpretation of intensity difference SAR images.....	29
3.3 How to display and view intensity difference SAR images.....	32
3.4 Flow of the image interpretation survey of sediment disasters by means of intensity difference SAR images.....	33
3.5 Checklist of the image interpretation survey of sediment disasters by means of intensity difference SAR images.....	37
4. Application of the image interpretation survey of sediment disasters by means of SAR images.....	41
4.1 Efficient method of image interpretation survey.....	41
4.2 Method of image interpretation survey that increases the reliability of results.....	43

5. Precautions for the techniques for the image interpretation survey of sediment disasters by means of SAR images.....	45
5.1 Effects of artificial modification	45
5.2 Orientation of a slope relative to the direction of microwave irradiation	47
 Part 3 Results of application of the image interpretation survey of sediment disasters by means of intensity difference SAR images	 49
1. Time required for the image interpretation survey of sediment disasters by means of intensity difference SAR images.....	49
2. Accuracy of the image interpretation survey of sediment disasters by means of intensity difference SAR images	50
2.1 Conditions of verification of accuracy	50
2.2 Results of verification of accuracy.....	52
References	56
Parameters of the SAR images in the text	57
Reference material 1. Time required for the image interpretation survey of sediment disasters by means of intensity difference SAR images of each disaster	58
Reference material 2. Accuracy of the image interpretation survey of sediment disasters by means of intensity difference SAR images in each disaster	66
Reference material 3. Checklist of the image interpretation survey of sediment disasters by means of intensity difference SAR images	71

Part 1 Basics concerning Synthetic Aperture Radar (SAR) images

1. Synthetic Aperture Radar (SAR)

1.1 Principles of SAR observation

The "Synthetic Aperture Radar" mounted on a satellite irradiates microwaves obliquely downward in the direction perpendicular to the traveling direction (azimuth direction) of the satellite (range direction) (Fig.-1.1.1).

The angle formed by the vertically downward direction of the satellite and the direction of microwave irradiation of the satellite is called the "off nadir angle," and the angle formed by the direction of microwave irradiation of the satellite when viewed from the direction of the apex of the target is the "incidence angle" (Fig.-1.1.1). Many satellites make the off nadir angle during observation variable, and on a inclined land, as shown in Fig.-1.1.2, the angle formed by the normal to the slope and the direction of microwave irradiation is called the "local incidence angle." Note that the relationship of "Off nadir angle < Incidence angle" holds even on a flat land because the Earth is a globe.

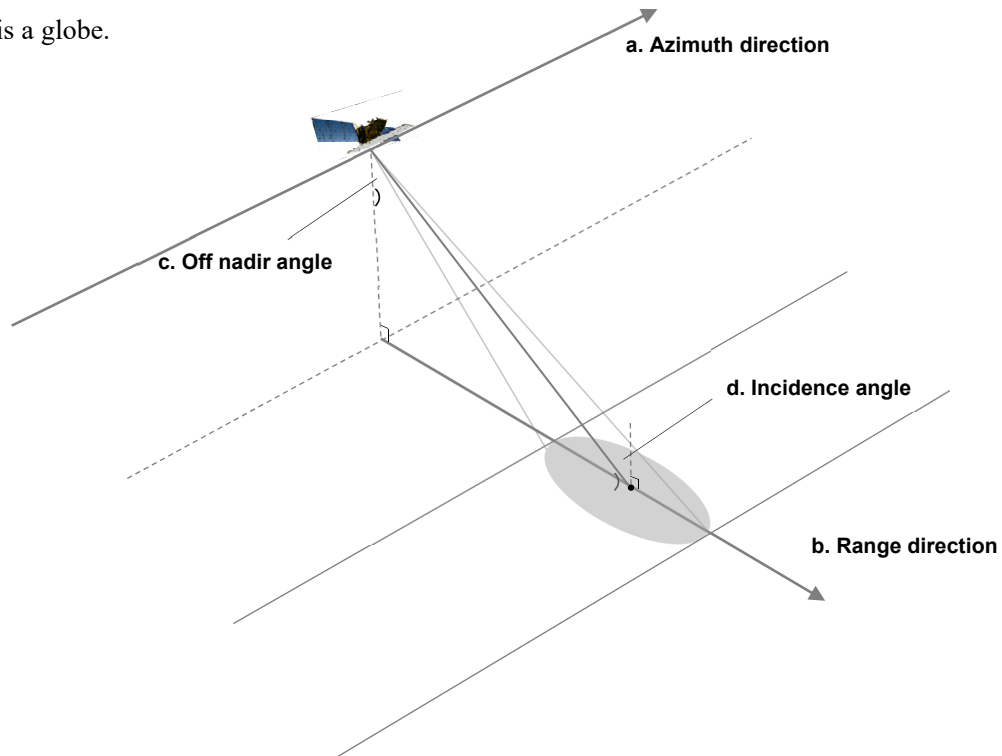


Fig.-1.1.1 Terms and a schematic diagram related to SAR observation

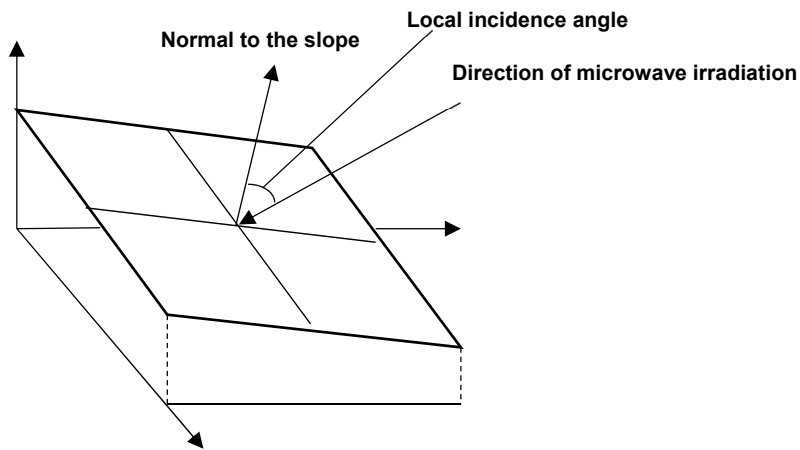


Fig.-1.1.2 Local incidence angle

The synthetic aperture technique realizes effects equivalent to those of the results of observation with a virtual antenna (synthetic aperture length (D_s)) having a length greater than the physical length of the antenna (actual aperture length (D_r)), by performing continuous observations that utilize the stable high-speed traveling of a satellite, etc. (Fig.-1.1.3). Also, theoretically the azimuth space resolution of SAR has a value half of the actual aperture length (D_r), and high-resolution observation data can be obtained.

Also, SAR is an image radar, which is a sensor for imaging (generating the image of) the target of observation.

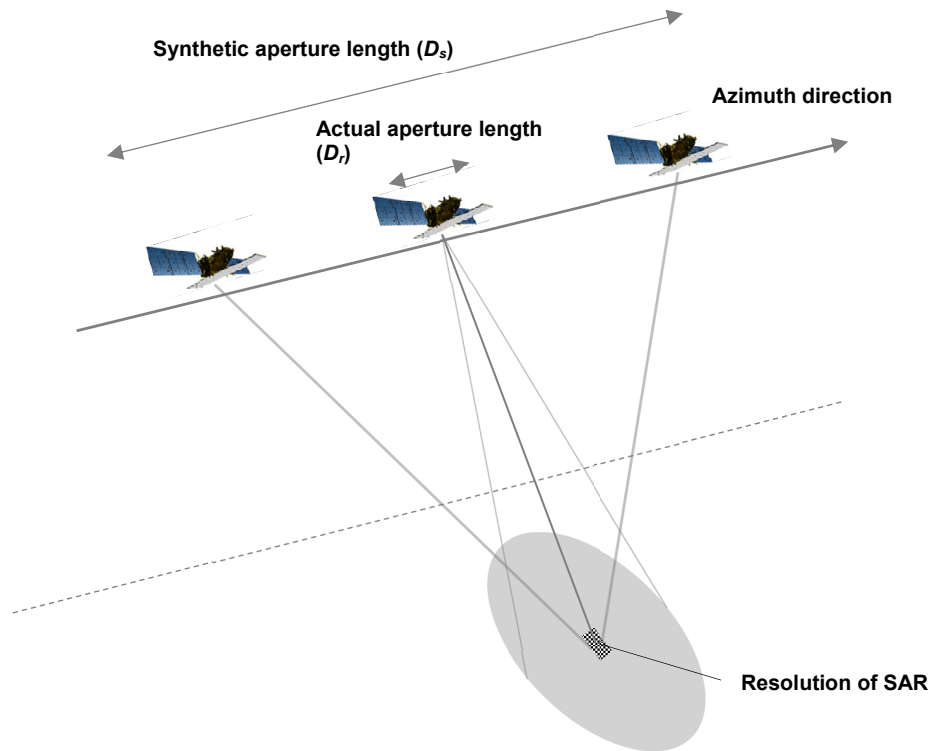


Fig.-1.1.3 Principles of the synthetic aperture technique

1.2 Features of SAR

Observation with SAR uses an active sensor that irradiates microwaves from the antenna itself of the radar to the target of observation, and receives the electromagnetic energy scattered by the target of observation with the antenna. Since it is not a passive sensor that utilizes the electromagnetic energy radiated by the sun, observation can be made day and night. Also, SAR is unlikely to be affected by cloud coverage, etc. because it irradiates microwaves (Fig.-1.1.4) having a wavelength greater than the size of a particle in the atmosphere such as cloud or rain.

Thus, SAR has an advantage of "all weather capability," thereby providing the merits of performing observation without depending on the time zone or meteorological condition.

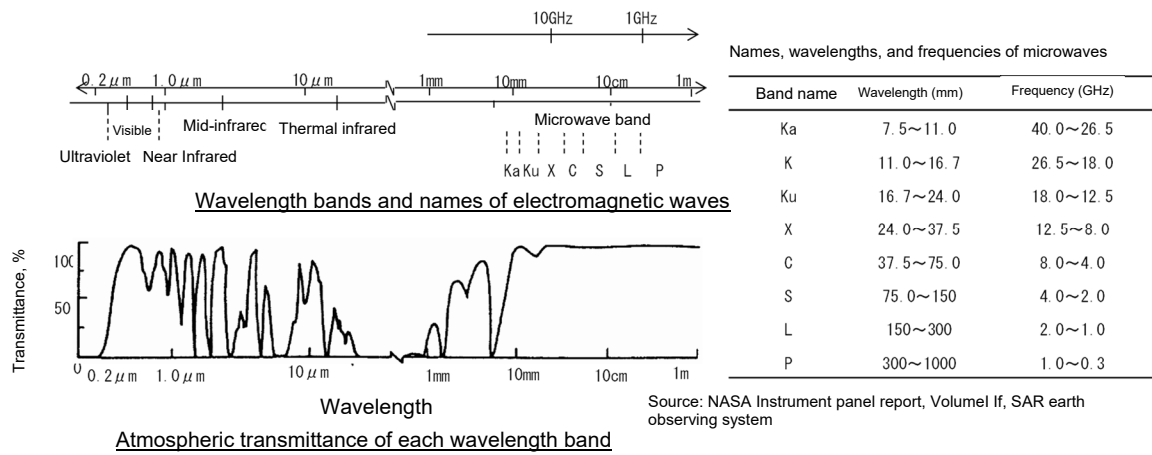


Fig.-1.1.4 Relationships between microwaves and atmosphere/cloud/rain

Source: Remote Sensing Technology Training Textbook "Microwave Remote Sensing"

From 1. Features of microwaves Relationships between microwaves and atmosphere/cloud/rain (created/edited by RESTEC)

1.3 Wavelength (band)

As SAR, microwaves (wavelength: approx. 0.1 to 100 cm) are used among the electromagnetic waves. They are subdivided into the band names shown in Fig.-1.1.5 according to the wavelength.

Microwaves with a relatively short wavelength such as those of the X band are scattered on a grassland, tree canopy, or on the surface of a leaf of a tree. On the other hand, if the wavelength is great such as that of the L band, the microwaves are transmitted through the grass land or tree canopy, and are scattered on the tree trunk or ground surface. Differences in the scattering characteristics depending on the wavelength will be described in "Part 1, 1.4 Scattering characteristics."

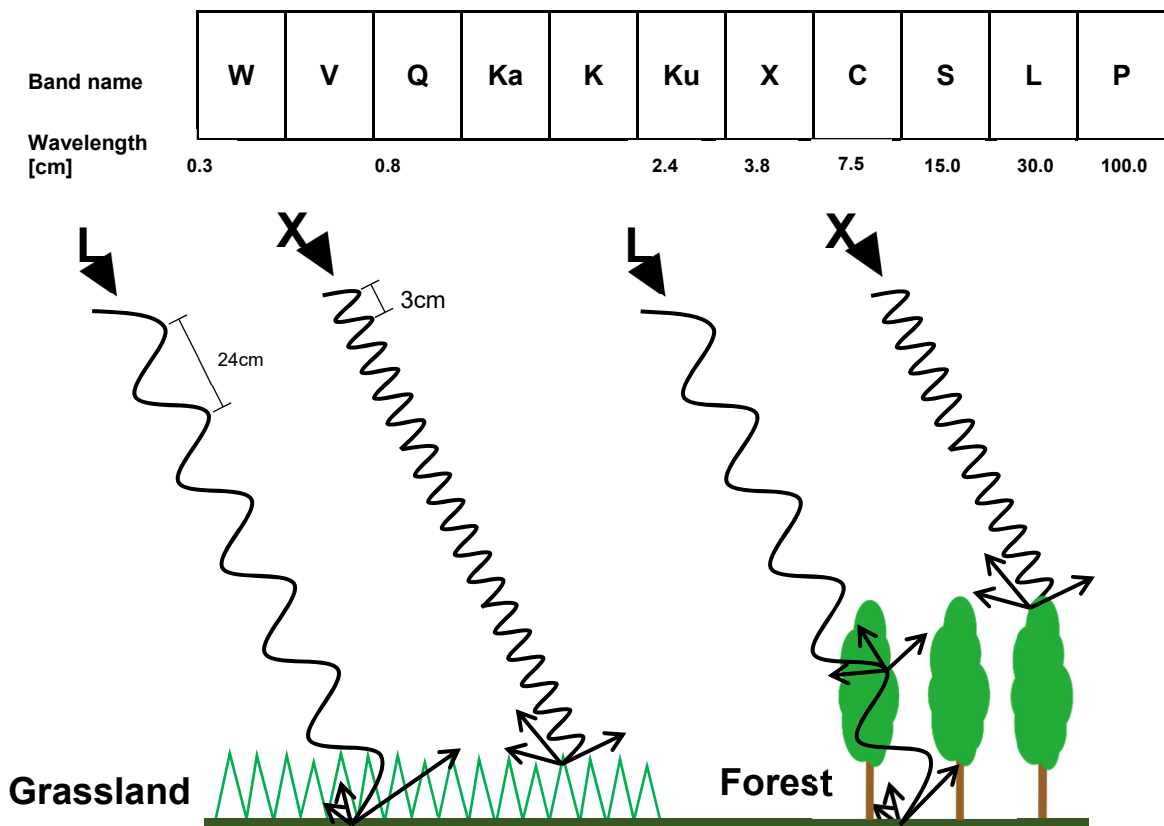


Fig.-1.1.5 Band names as well as classification and features of wavelengths

1.4 Scattering characteristics

The intensity of microwaves returning to the irradiation direction side after the irradiated microwaves have been scattered on the ground surface, etc. is called the "backscatter intensity," which is recorded as the "backscatter coefficient" in the SAR observation data. The backscatter coefficient has dependency on the incidence angle, according to the roughness of the scattering surface.

The backscatter coefficient is described as follows.

Let P_t be the transmitted power, λ the wavelength, R the distance from the antenna, G the antenna gain, and σ the cross-sectional area of the radar. Since SAR performs the transmission and receiving of radio waves by means of a single antenna, the monostatic radar equation is applied, and the received power P_r is represented by Equation-1.1.1.

$$P_r = \frac{P_t G^2 \lambda^2}{(4\pi)^3 R^4} \sigma \quad \text{Equation-1.1.1}$$

Since the backscatter coefficient (σ^0) is the cross-sectional area (σ) of the radar per unit area (A) on the scattering surface, it is represented by Equation-1.1.2.

$$\sigma^0 = \frac{P_r (4\pi)^3 R^4}{P_t G^2 \lambda^2 A} \quad \text{Equation-1.1.2}$$

1.4.1 Surface scattering

The scattering of microwaves irradiated from SAR on the border surface such as the ground surface is called "surface scattering." Surface scattering is affected by the roughness on the border surface. There are characteristics such that, when the microwaves are irradiated to a smooth surface, scattering toward the side opposite to the direction of irradiation (forward scatter) increases, and when irradiated to a rough border surface, scattering toward the side of the direction of irradiation (backscatter) increases (Fig.-1.1.6).

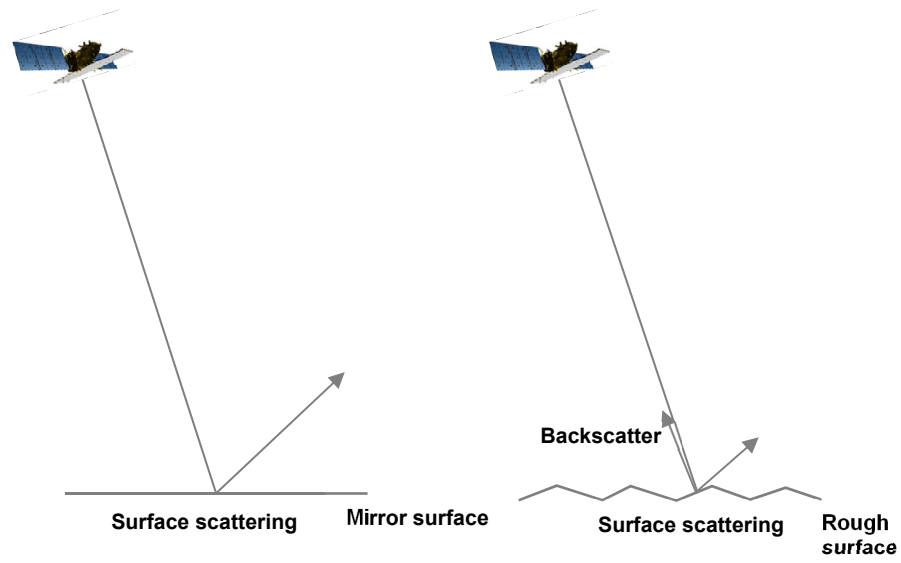


Fig.-1.1.6 Schematic diagram of surface scattering

1.4.2 Volume scattering

The occurrence of scattering caused by unevenness of the internal inductive capacities as a result of the propagation of microwaves irradiated from SAR by penetrating the border part is called "volume scattering." Since it is a phenomenon caused by penetration of the microwaves to the inside, attention should be paid to it when handling microwaves having a great wavelength and when observing a target with a smooth border surface having a low inductive capacity where surface scattering is unlikely to occur.

In the case of L-band, a typical example is volume scattering inside a forest, and volume scattering in the inside of a tree and surface scattering on the ground surface need to be considered simultaneously (Fig.-1.1.7; on the left).

1.4.3 Double-bounce scattering

As shown in Fig.-1.1.7 on the right, there is a phenomenon called "double-bounce scattering" in which backscatter increases as a result of recurrence of scattering after surface scattering has occurred. It may occur strongly in cases such as those where the direction of microwave irradiation comes face-to-face with a building, structure, etc.

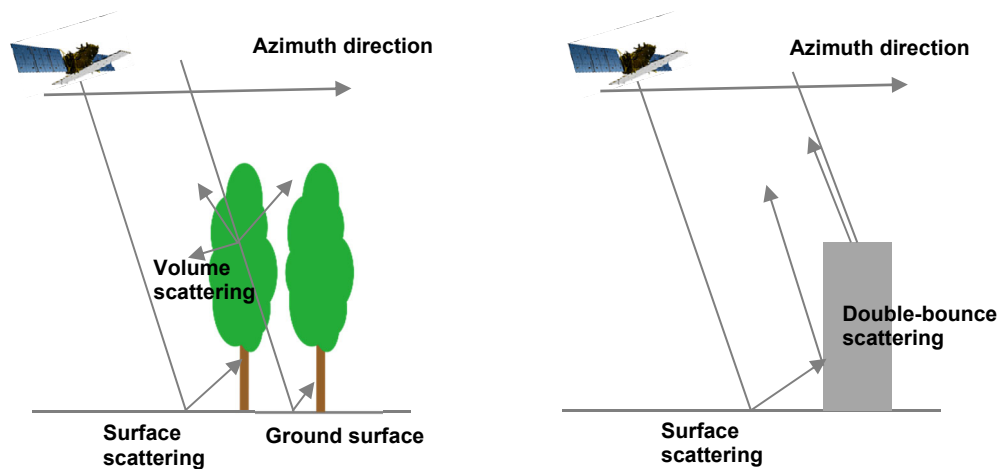


Fig.-1.1.7 Schematic diagrams of volume scattering and double-bounce scattering

1.5 Polarization characteristics

Electromagnetic waves are classified by the surface containing the direction of the electric field (polarization surface) into horizontal polarization (of which amplitude has a horizontal surface relative to the direction of propagation: H) and vertical polarization (of which amplitude has a vertical surface relative to the direction of propagation: V) (Fig.-1.1.8), and are expressed as HH, HV, VH, and VV by the combination of transmission and receiving (1st letter: irradiation, 2nd letter: receiving).

When electromagnetic waves are reflected or scattered, the state of polarization may vary depending on the geometrical shape of the target. SAR that uses microwaves have features such that images generated by horizontal polarization are different from those generated by vertical polarization.

The characteristics are such that, when horizontal polarization (H) has been irradiated to a target having a cubic structure like a forest, part of it rotates and is reflected as vertical polarization (V), and in the case of vertical polarization (V) having being irradiated as well, part of it is reflected as horizontal polarization (H). HH and VV are called "like-polarization," and these polarization characteristics reduce backscatter of the observation target whose volume scattering is dominant such as a forest. On the other hand, HV and VH are called cross-polarization, which increases backscatter of a forest, etc.

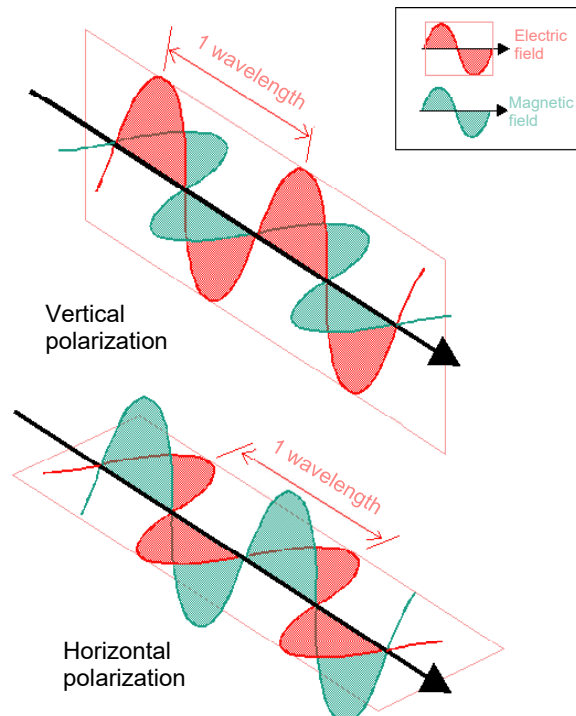


Fig.-1.1.8 Schematic diagrams of horizontal polarization and vertical polarization

Source: Remote Sensing Technology Training Textbook "Microwave Remote Sensing"
From 3-2. Features of SAR images Polarimetry (created/edited by RESTEC)

2. SAR images

2.1 Generation of SAR images

"SAR images" are the data of the darkness levels according to the backscatter intensity at each point on the ground surface that has been observed by SAR that have been visualized as each pixel. SAR images that show the backscatter intensity of certain polarization are called "single-polarized SAR images."

Fig.-1.2.1 shows single-polarized SAR images. From the single-polarized SAR images, topographical features can be identified that are like a scarp having a horseshoe shape. Also, in the channel of the river flowing in the northern and southern directions that is located right under the scarp, light colors are dominant signifying that backscatter is intense, where Sediment deposition may have occurred. Moreover, a range can slightly be identified in the upstream side (north side) of the colluvial soil that is considered to be an inundated area, where backscatter is shown with a dark color to be considerably low, and it is conjectured that there is a situation where a natural dam has been formed by channel blockage.

As stated above, locations of channel blockage that have been caused by a large-scale slope failure, etc. of roughly 10,000 m² or more in planar projection area can often be extracted by the image interpretation of topography using single-polarized SAR images having a high spatial resolution. For details, refer to NILIM Technical Note No. 760.

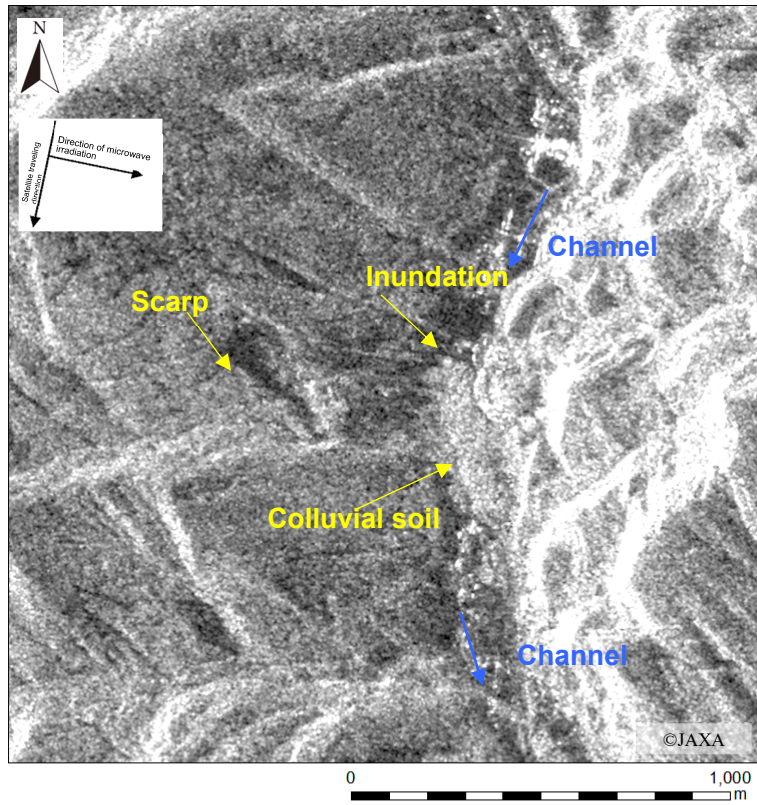


Fig.-1.2.1 Example of a single-polarized SAR image (Hita City, Oita Prefecture)

2.2 Features of SAR images

Due to the factors described above in "Part 1, 1.1 Principles of SAR observation," SAR images provides a look like a bird's-eye view having distortion (projecting the topography as though it has fallen down). Also, the backscatter intensities visualized in SAR images are shown in darkness corresponding to the land cover that becomes a scattering surface or its texture, and therefore intuitive interpretation of the target of observation is difficult. In the single-polarized SAR images in Fig.-1.2.2, the bent part of the Iya River is conspicuously distorted, and it is difficult to distinguish forests from farmland, etc.

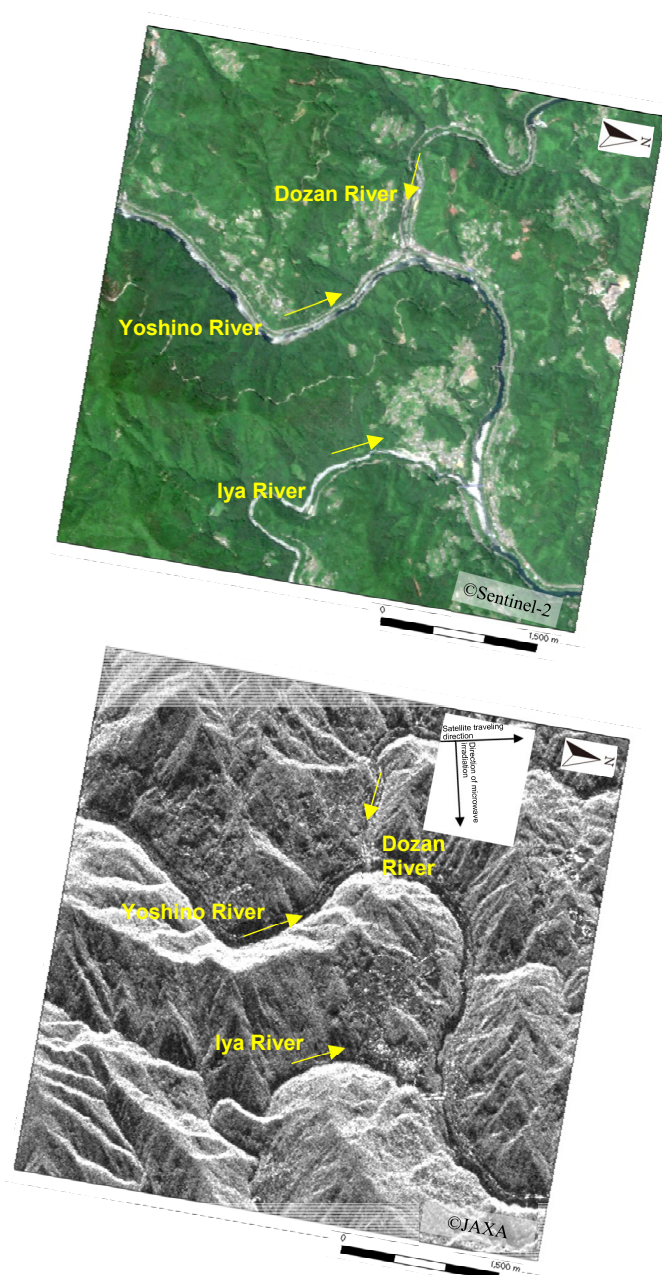


Fig.-1.2.2 Differences in appearance between an optical image (top) and a single-polarized SAR image (bottom) (Miyoshi City, Tokushima Prefecture)

2.3 Precautions for SAR images

Due to the fact that the direction of microwave irradiation that was described above in "Part 1, 1.1 Principles of SAR observation" is obliquely downward and due to geometrical relationships with the topography, in the SAR images, distortion may occur or an invisible range resulting from such distortion may occur. This effect is collectively called the "geometric image modulation"; the following 3 points will be explained.

2.3.1 Foreshortening

The position of the target to be observed on an image in SAR is determined by the time of reciprocation required for the transmission and receiving of microwaves. If the target to be observed has a height, it is projected toward the front side according to the shortened portion of the transmission and receiving time of microwaves, and the target having an altitude on the SAR image appears to have fallen down toward the side of irradiation direction of the microwaves. This phenomenon is called "foreshortening."

When an explanation is given by taking Mt. Fuji shown in Fig.-1.2.3 as an example, Point A that shows the mountain top of a mounting having a high altitude is projected as though falling down to the position of Point A' at the side of the direction of microwave irradiation (west side) as compared with the actual position. On the other hand, a place with a low altitude is affected little by foreshortening, and the actual position of Point B is almost the same as the position of the projected Point B'.

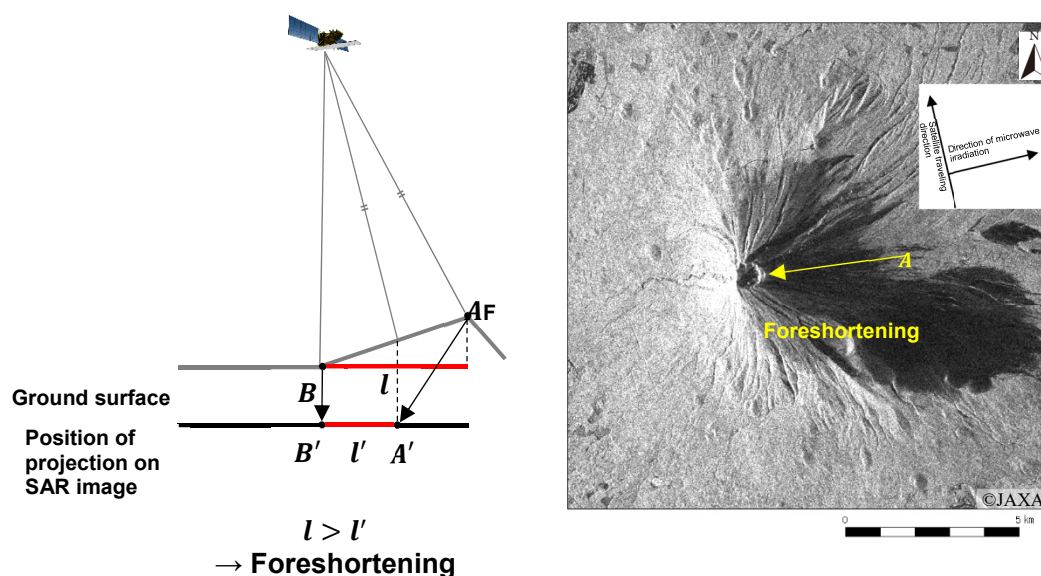


Fig.-1.2.3 Schematic diagram of foreshortening and an example by means of a single-polarized SAR image (around Mt. Fuji)

2.3.2 Layover

If the degree of inclination of a slope increases, the effects of foreshortening become greater, and the positional relationships between the top end and bottom end of the slope may be projected in a reversed manner. This phenomenon is called "layover."

When an explanation is given by taking Mt. Fuji shown in Fig.-1.2.4 as an example, Point *A* at the mountain top of Mt. Fuji is greatly subjected to foreshortening toward the west side, and is projected to Point *B* on the slope at the west side as though covering Point *B*, and the slope at the west side (section *AB-BC*) becomes an invisible range widely. Also, since scattering is dense on the slope at the west side where layover occurs, SAR images are featured by being displayed in conspicuously light colors as though there are great backscatter intensities.

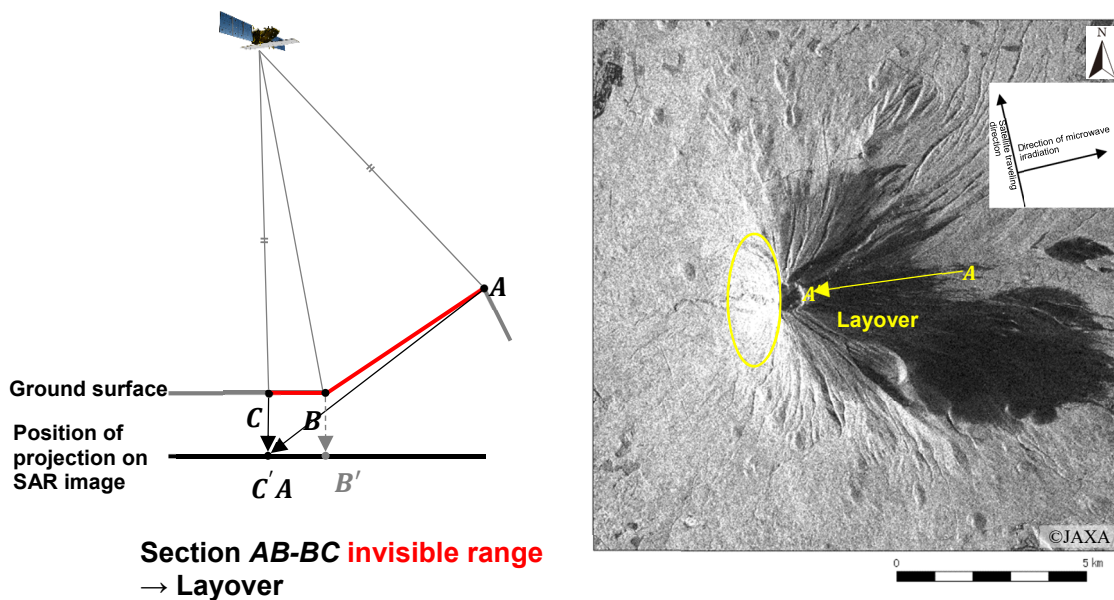


Fig.-1.2.4 Schematic diagram of layover and an example by means of a single-polarized SAR image (around Mt. Fuji)

2.3.3 Radar shadow

In a place where microwaves are not irradiated shadowed by the slope, scattering does not occur at all, and projection is done on SAR images as if shadowing effects have been produced. This is called "radar shadow," and this range is invisible. When the off nadir angle increases, the range where radar shadow occurs also is expanded.

When an explanation is given by taking Mt. Fuji shown in Fig.-1.2.5 as an example, on the slope at the east side from mountain top *A* of Mt. Fuji, microwaves do not reach the ground surface, and radar shadow occurs. Since there are no scattered microwaves in the radar shadowed part, on SAR images, backscatter is shown in dark colors where the backscatter is considerably low. Since its visibility is similar to surface scattering that occurs on a smooth, flat land area such as water surface, attention should be paid to its distinction.

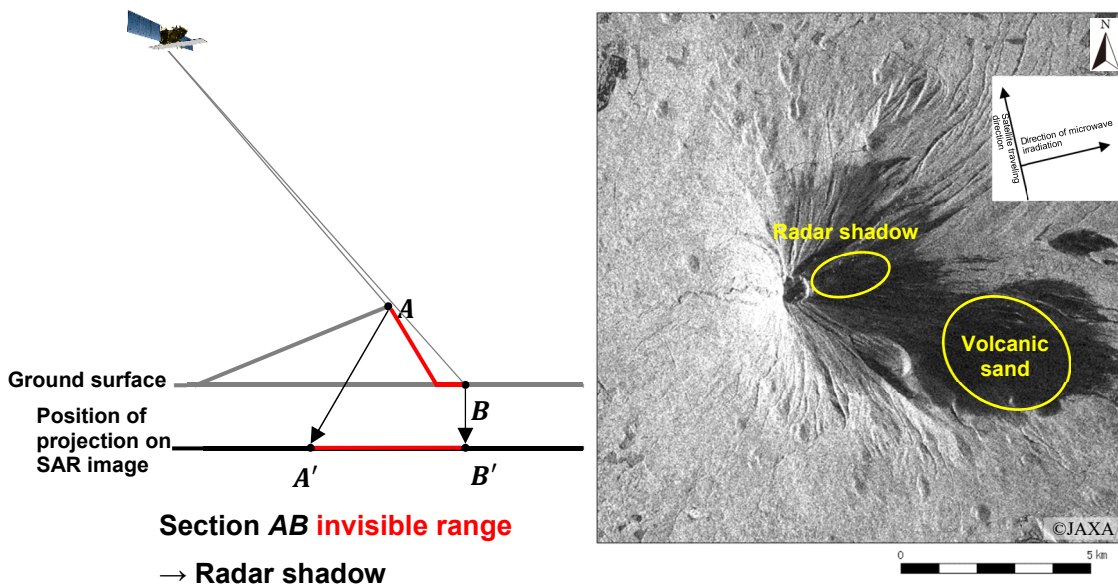


Fig.-1.2.5 Schematic diagram of layover and an example by means of a single-polarized SAR image (around Mt. Fuji)

2.4 Resolution of SAR images

When the distance between 2 points, Point A and Point B, is sufficient, scattered microwaves can be distinguished at each point, but when the positional relationship between Point A and Point B is closer, each scattering situation cannot be distinguished (Fig.-1.2.6). The limit distance between 2 points that enables this distinction is called resolution.

However, the resolution of SAR images and the size of the target of observation that can be distinguished are different from each other, and generally it is considered that in order to visually identify a specific target, its size needs to be 10 - 20 times the resolution.

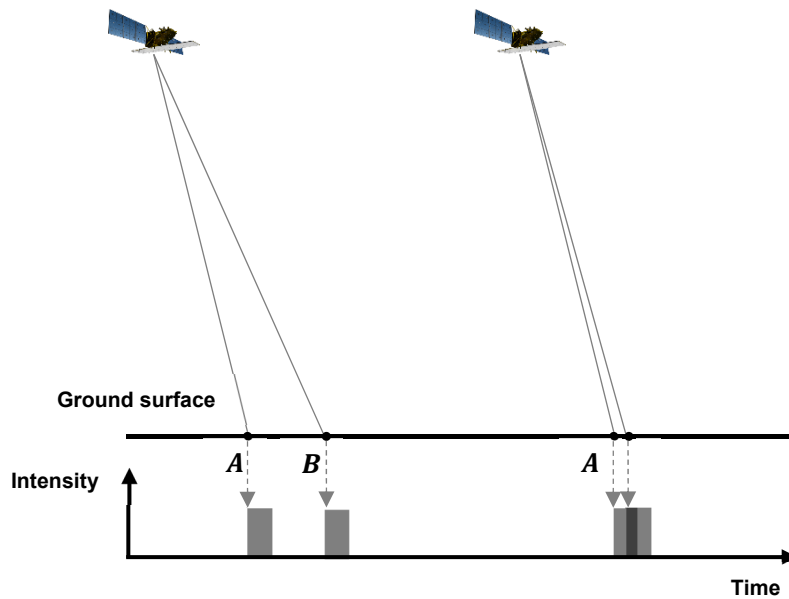


Fig.-1.2.6 Schematic diagram of resolution

The resolution R [m] of SAR images is shown by Equation 1.2.1, and theoretically the greater the incidence angle, the higher the resolution.

$$R = \frac{c}{2B \sin \theta} \quad \text{Equation-1.2.1}$$

c [m/s]: Speed of microwaves in air (speed of light), B [Hz]: Bandwidth of chirp signals, θ [°]: Incidence angle

2.5 Analysis and types of SAR images

By synthesizing multiple polarized SAR images or by comparing SAR images that have been observed in different periods, SAR images are generated that enable the situation of ground objects and ground surface cover to be distinguished at a higher level. This material handles the 3 types of SAR images shown in Table-1.2.1.

Table-1.2.1 Types and features of SAR images to be handled in this material

Type	Features
Single-polarized SAR images	<ul style="list-style-type: none"> • Visualize the backscatter intensity of single-polarization in 1 period • Image expressed in darkness
Dual-polarized SAR images	<ul style="list-style-type: none"> • Visualize the differences in scattering characteristics of each polarization in 1 period • Spatial resolution is lower than that of single-polarized SAR images
Intensity difference SAR images	<ul style="list-style-type: none"> • Visualize the changes in backscatter intensity of single-polarization in different periods • Single-polarized SAR images under the same conditions except for the observation period are required

2.5.1 Single-polarized SAR images

Single-polarized SAR images are the basic darkness images that express the scattering intensity of microwaves. Aside from HH, single-polarized SAR images of each of the polarization components, HV, VV, and VH can be generated. Note that the single-polarized SAR images of HH polarization are shown above in Fig.-1.2.1.

Single-polarized SAR images enable the rough situation of topography and ground surface cover to be grasped from the darkness that shows the backscatter intensity. In particular, since water areas have features such that the backscatter intensity becomes considerably low, an inundated area in a channel area caused by the formation of a natural dam may be interpreted.

2.5.2 Dual-polarized SAR images

Dual-polarized SAR images are images in which the anisotropy of the scattering characteristics of 2 types of polarization is visualized. They can be created by RGB color synthesis processing of single-polarized SAR images of like-polarization and single-polarized SAR images of cross-polarization.

Fig.-1.2.7 shows dual-polarized SAR images that have been created by RGB color synthesis processing with R (red): HH polarization, G (green): HV polarization, and B (blue): HH polarization, according to NILIM Technical Note No. 791. The forest areas are expressed in green, and bare land without forests is expressed in purple red, thereby making it possible to distinguish forests and bare land including failure areas based on the image color.

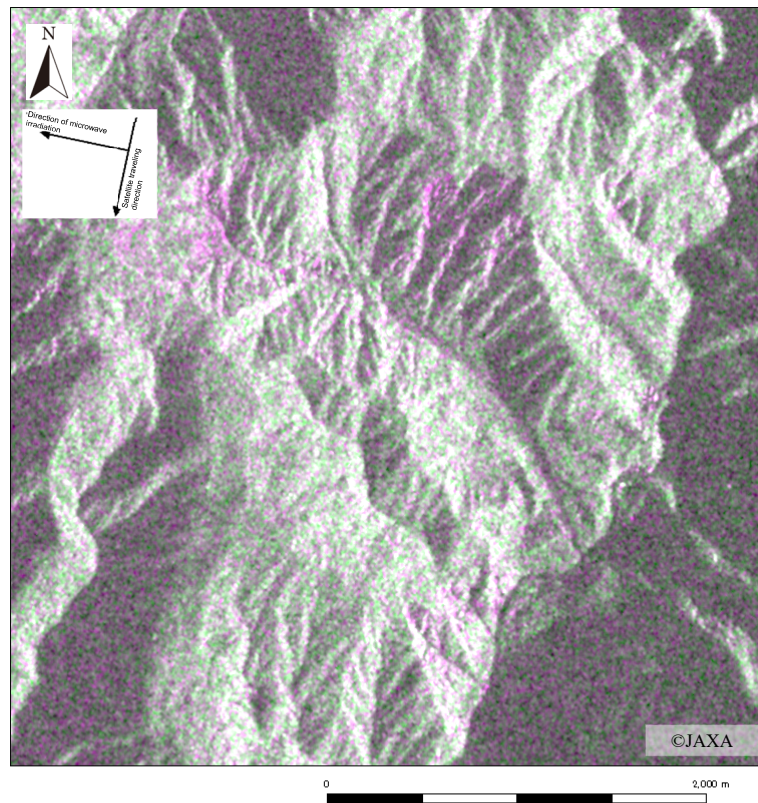


Fig.-1.2.7 Example of a dual-polarized SAR image (Aoi Ward, Shizuoka City, Shizuoka Prefecture)

2.5.3 Intensity difference SAR images

Intensity difference SAR images are images in which changes in the backscatter intensity between single-polarized SAR images that have been observed in different periods are visualized. They can be created by RGB color synthesis processing of 2 single-polarized SAR images under the same conditions of observation except for the observation period.

In this material, intensity difference SAR images are created by assigning R (red): archive images, G (green): new observation images, and B (blue): new observation images (Fig.-1.2.8). In the 2 periods, the place where the backscatter intensity decreased is expressed in red, and the place where the backscatter intensity increased is expressed in cyan (greenish-blue close to light blue), thereby making it possible to distinguish the situation of occurrence of a sediment disaster based on the change in image color.

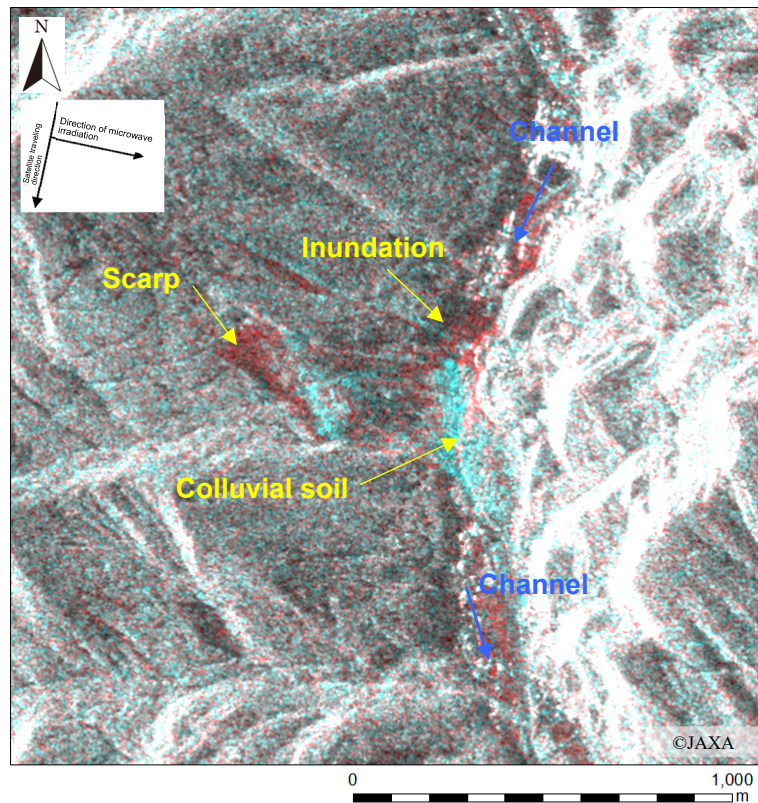


Fig.-1.2.8 Example of an intensity difference SAR image (Hita City, Oita Prefecture)

3. Utilization of SAR images in the image interpretation survey of sediment disasters

3.1 Conditions of observation of SAR images suitable for the image interpretation survey of sediment disasters

As described above in "Part 1, 2.2 Features of SAR images, 2.3 Precautions for SAR images," in SAR images, there exists an invisible range caused by characteristic distortion resulting from observation principles and the falling down of topography. The effects of this invisible range can be partially reduced by considering the conditions of observation. Table-1.3.1 shows the conditions of observation of SAR images suitable for the image interpretation survey of sediment disasters.

Table-1.3.1 Conditions of observation of SAR images suitable for the image interpretation survey of sediment disasters

Conditions of observation	Recommended value
Off nadir angle	About 30° - 45°
Resolution	to about 3 m
Wavelength (band)	About 3 - 30 cm (X/C/L)

When the off nadir angle decreases, the effects of layover increase, and when the off nadir angle increases, the effects of radar shadow increase. For this reason, it is appropriate to use SAR images that have been observed at an off nadir angle of about 30° - 45° in a mountainous area to which the image interpretation survey of sediment disasters is applicable.

In general, it is desirable to utilize SAR images with higher resolution in the image interpretation survey of sediment disasters, because the distinction of ground objects and ground surface cover will be easier. This material explains techniques for the image interpretation survey of sediment disasters that have been verified by using SAR images of about 3 m in resolution.

When distinguishing the occurrence of a sediment disaster, the difference in visibility in the X- to L-band is small. Therefore, the techniques for the image interpretation survey of sediment disasters to be explained in this material assume that SAR images that have been observed in the X- to L-band can be utilized.

3.2 Precautions when utilizing SAR images in the image interpretation survey of sediment disasters

3.2.1 Invisible ranges in SAR images

As described above in "Part 1, 2.3 Precautions for SAR images," there exists in SAR images an invisible range due to the occurrence of falling down, etc. of topography. In a mountainous area to which the image interpretation survey of sediment disasters is applicable, this effect appears more conspicuously.

Fig.-1.3.1 shows the situation of occurrence of a sediment disaster in contrast to the visibility of intensity difference SAR images. Thus, it is necessary to handle the results of image interpretation survey, with an awareness of the direction of microwave irradiation and the slope direction, by paying attention to the fact that there is a range where the image interpretation of failure areas is disabled in the image interpretation survey of sediment disasters by means of SAR images.

Note that this invisible range occurs irrespective of the type of SAR images described in "Part 1, 2.5 Analysis and types of SAR images."

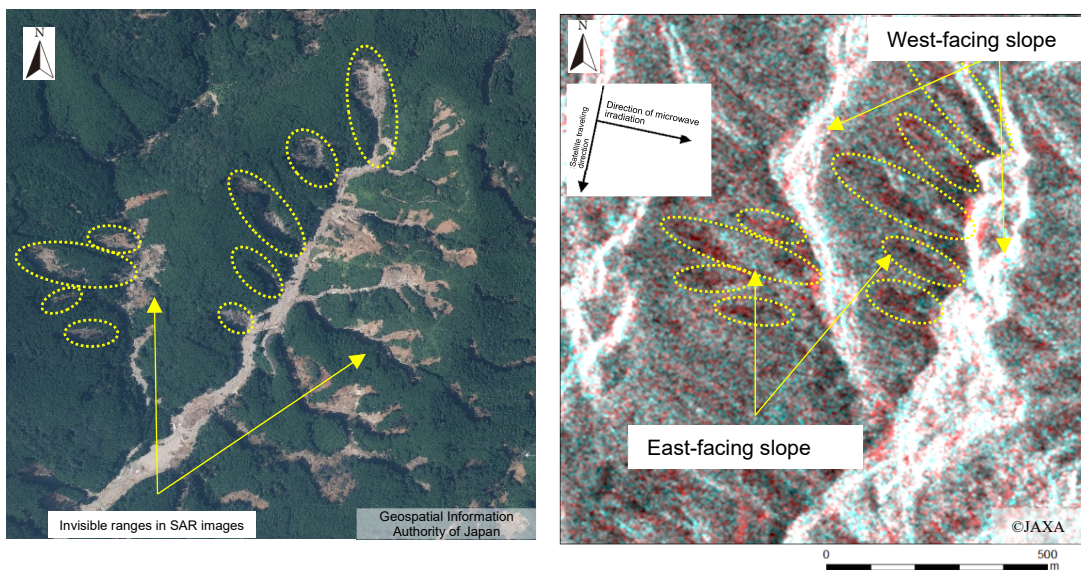


Fig.-1.3.1 An example of invisible ranges in SAR images (Asakura City, Fukuoka Prefecture)

3.2.2 Problems in ground object identification by means of SAR images

When implementing the image interpretation survey of sediment disasters for mountainous areas, some polarization characteristics obtained from SAR images and changes in the backscatter intensity show places with aspects that are similar to those of the occurrence of sediment disasters, and interpretation may be done by misreading.

With dual-polarized SAR images, it is difficult to distinguish the places with sediment disasters from bare land such as deforested area or land where a failure already occurred (Fig.-1.3.2), and with intensity difference SAR images, attention needs to be paid to artificial modification (deforestation, topography modification, etc.) and seasonal changes (inundation of farmland, etc.) in the 2 periods (Fig.-1.3.3). Interpretation of changes in intensity difference SAR images will be described in detail in Part 2.

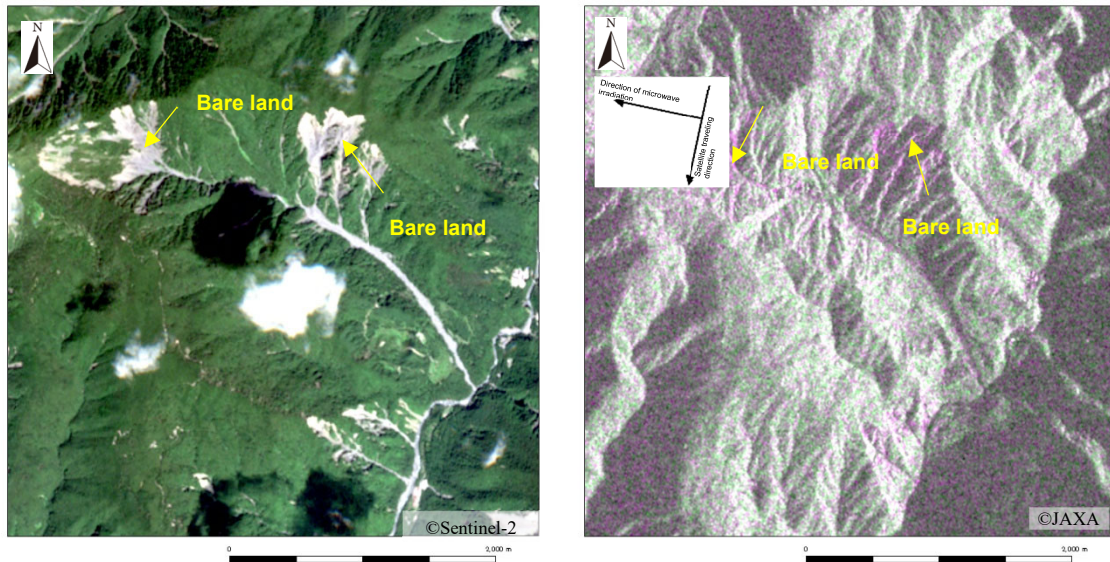


Fig.-1.3.2 Appearance of bare land in dual-polarized SAR images
(Aoi Ward, Shizuoka City, Shizuoka Prefecture)

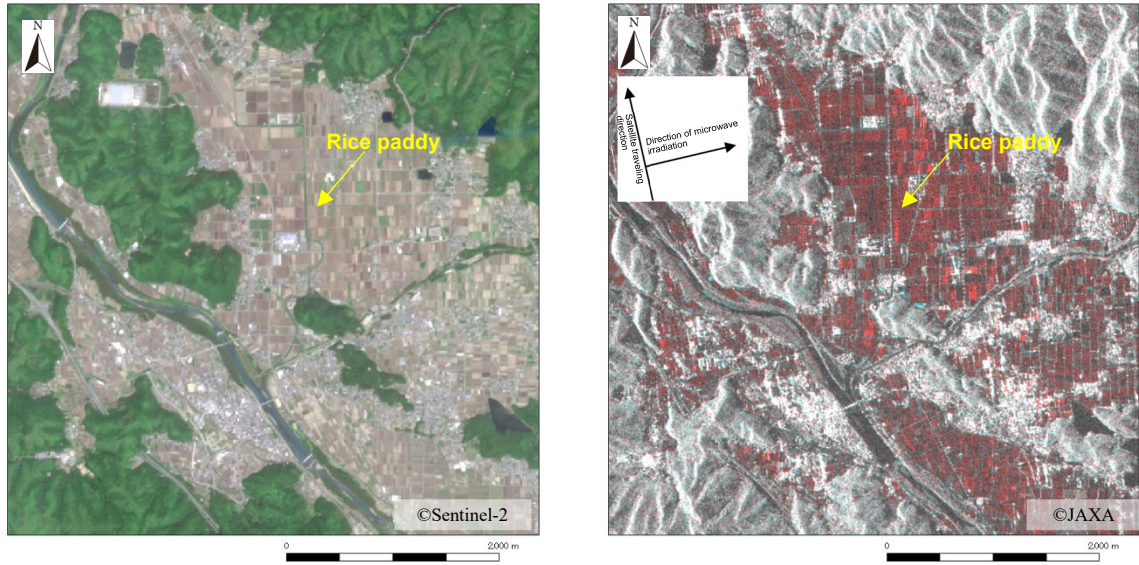


Fig.-1.3.3 Appearance of rice paddies in intensity difference SAR images (Nantan City, Kyoto Prefecture)

Part 2 Explanations of the techniques for the image interpretation survey of sediment disasters by means of SAR images

1. Selection of the techniques for the image interpretation survey of sediment disasters by means of SAR images

1.1 Selection according to the conditions of available SAR images

When selecting the techniques for the image interpretation survey of sediment disasters by means of SAR images, judgment is made as to which will be used, dual-polarized SAR images or intensity difference SAR images, according to the conditions of observation, etc. of available single-polarized SAR images. This SAR image selection flow is shown in Fig.-2.1.1.

In the first place, the range of implementation of the image interpretation survey of sediment disasters is selected. Next, the results of observation of SAR that include the range of survey are searched, and it shall be checked whether new observation under the same conditions of observation as those in the archive is possible.

If possible, a request for observation is made under the same conditions of observation, and single-polarized SAR images by means of the archive and new observation are obtained. By using these, intensity difference SAR images are generated and the image interpretation survey of sediment disasters is implemented.

If new observation cannot be made under the same conditions of observation as those of the archive, a request for observation by means of dual-polarization is made, and the SAR data of such observation are obtained. From the SAR observation data of dual-polarization, dual-polarized SAR images are generated, and the image interpretation survey of sediment disasters is implemented.

Note that search of the archive and the request for observation need to be checked with the operator, data handling personnel, etc. of the applicable SAR.

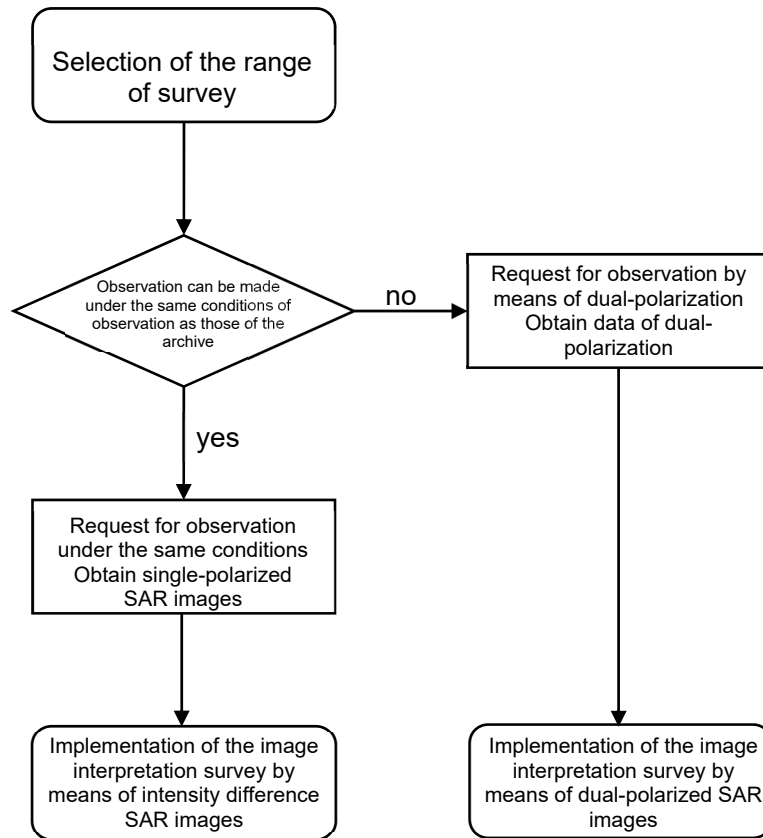


Fig.-2.1.1 Selection flow of the techniques for the image interpretation survey of sediment disasters according to the conditions of available SAR images

1.2 Selection according to the scale of a sediment disaster to which the image interpretation survey is applicable

Selection is possible according to the scale of a sediment disaster to which the image interpretation survey is applicable (Table-2.1.1).

According to NILIM Technical Note No. 791, it is considered that dual-polarized SAR images can be applied to the interpretation of a large-scale failure and channel blockage of roughly 10,000 m² or more. With intensity difference SAR images, results have been obtained in which a large-scale failure and channel blockage of 10,000 m² or more can be detected with a high degree of certainty, and a relatively small-scale failure of 2,000 m² or more can also be detected at a rate of around 70% (to be described in detail in Part 3). They can sufficiently be applied, when a surface layer failure, etc. has occurred with a high density, if the accuracy is such that the range and external edges of such failure are specified.

Therefore, if the conditions shown in "Part 2, 1.1 Selection according to the conditions of available SAR images" are satisfied, the image interpretation survey by means of intensity difference SAR images is recommended.

Table-2.1.1 Types of SAR images to be handled in this material

Techniques for the image interpretation survey of sediment disasters by means of SAR images	Large-scale failure Channel blockage	Small-scale failure
Image interpretation survey by means of dual-polarized SAR images	○ (Applicable)	× (Not applicable)
Image interpretation survey by means of intensity difference SAR images	○ (Detection of about 80%)	○ (A majority can be detected)

* Large-scale: area in orthographic projection 10,000 m² or more, small-scale: area in orthographic projection 2,000 m² or more

* The invisible range is not included in the scope of verification.

2. Image interpretation survey of sediment disasters by means of dual-polarized SAR images

By the interpretation of dual-polarized SAR images having a high spatial resolution, a large-scale slope failure or areas of channel blockage resulting from such failure may be extracted. For details, refer to NILIM Technical Note No. 791.

3. Image interpretation survey of sediment disasters by means of intensity difference SAR images

The image interpretation survey of sediment disasters by means of intensity difference SAR images is explained below, using examples of the 2018 Hokkaido Eastern Iburi Earthquake. Note that the image interpretation survey of sediment disasters hereafter assumes that the standard functions provided in GIS software and image processing software are utilized.

3.1 Generation of intensity difference SAR images

As for the intensity difference SAR images, as described above in Part 1, single-polarized SAR images that were observed before and after the disaster, respectively, are prepared, and then changes in the backscatter intensity are visualized. Two types of images have been obtained: the single-polarized SAR images that were observed before the occurrence of the earthquake (August 23, 2018) (archive) and the single-polarized SAR images that were newly observed right after the occurrence of the earthquake (September 6, 2018). By assigning R (red): August 23, 2018, G (green): September 6, 2018, and B (blue): September 6, 2018 to these images, intensity difference SAR images are generated by the RGB color synthesis processing (Fig.-2.3.1).

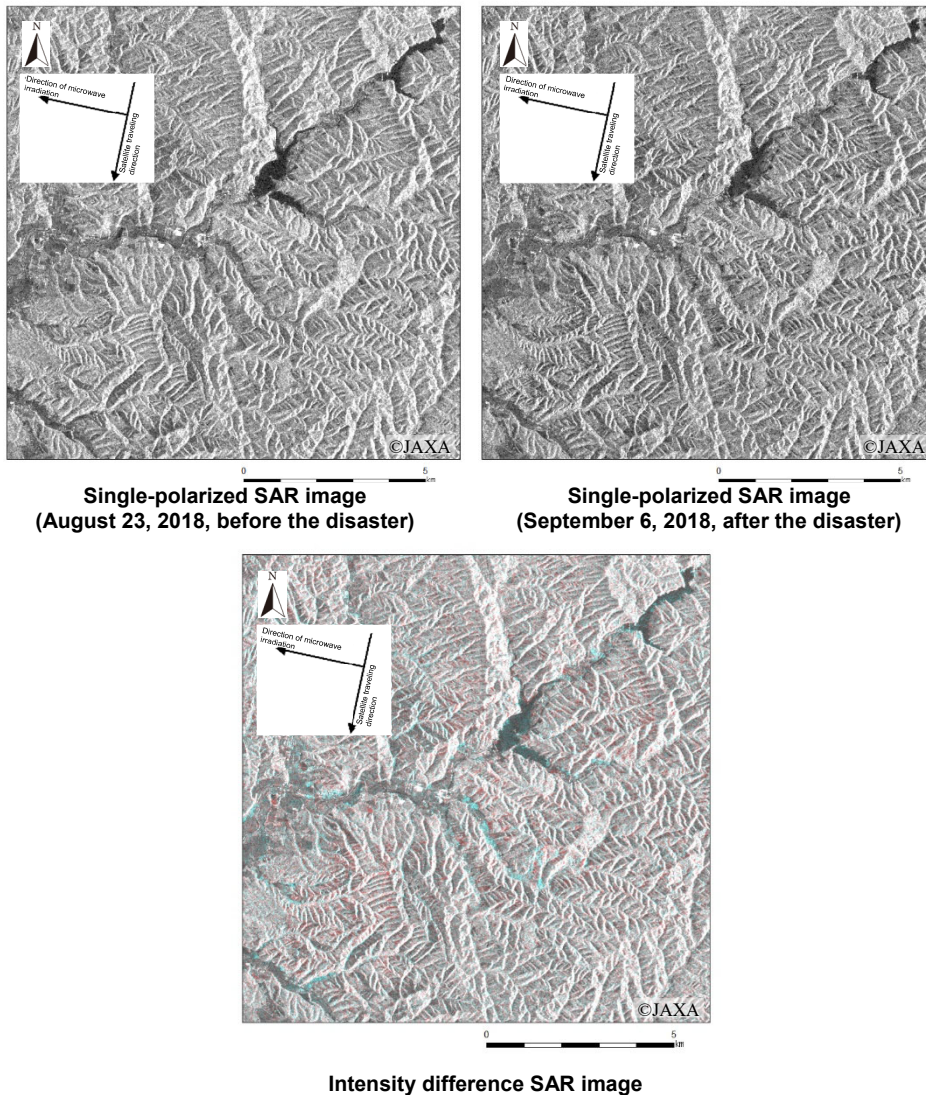


Fig.-2.3.1 Generation of intensity difference SAR images
 (Atsuma Town, Mukawa Town, Hokkaido Prefecture)

3.2 Interpretation of intensity difference SAR images

In the image interpretation survey of sediment disasters, places with inflow of failure sediment and with a high probability of slope failure are extracted from the color changes in the intensity difference SAR images that show changes in the backscatter intensity before and after the disaster. The relationships between changes in color and changes in the backscatter intensity on the intensity difference SAR images are shown in Table-2.3.1.

When there is no change in the backscatter before and after the disaster in a place where the backscatter is great in ordinary times such as a forest or farmland, it is displayed in white on the

intensity difference SAR images. Also, when there is no change in the backscatter before and after the disaster in a place where the backscatter is considerably small such as water areas on a sea surface, etc., it is displayed in black on the intensity difference SAR images. As shown in Fig.-2.3.2, if sediment flows in a rice paddy, etc. due to the occurrence of a disaster, the backscatter intensity increases after the disaster, and therefore the place is shown in cyan on the intensity difference SAR images, and in a place where outflow of a forest was caused by a slope failure, the backscatter intensity decreases after the disaster, and therefore the place is shown in red on the intensity difference SAR images.

Table-2.3.1 Changes in color and in backscatter intensity on intensity difference SAR images

Color	Changes in backscatter intensity before and after the disaster	Example
White	Backscatter intensity exists, and there is no change	Forest, farmland
Black	Backscatter intensity is small, and there is no change	Sea surface, lake surface
Cyan	Backscatter intensity increases after the disaster	Sediment outflow, floating object
Red	Backscatter intensity decreases after the disaster	Slope failure, water seepage/inundation

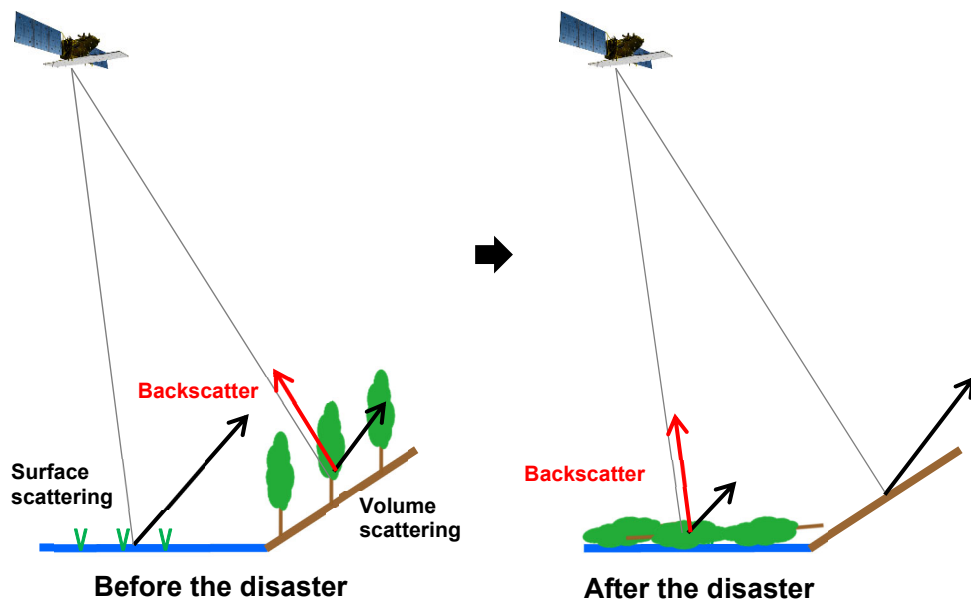


Fig.-2.3.2 Image of changes in backscatter intensity caused by the occurrence of a sediment disaster

When comparing the intensity difference SAR image with the optical image in Fig.-2.3.3, it is found that the red range on the intensity difference SAR image corresponds very well with the position of the failure area on the optical image. Due to the occurrence of the slope failure, forests, etc. have been lost and smooth failure surfaces have been exposed, with the result that the situation where the backscatter intensity has decreased as compared with that before the disaster has appeared distinctly. Also, the change in cyan that appears linearly on the intensity difference SAR image corresponds to the valley bottom plain area on the optical image. It is considered that, as a result of outflow of sediment, etc. from the failure onto the smooth, flat land area such as farmland, appearance is shown in which the backscatter intensity has increased as compared to that before the disaster.

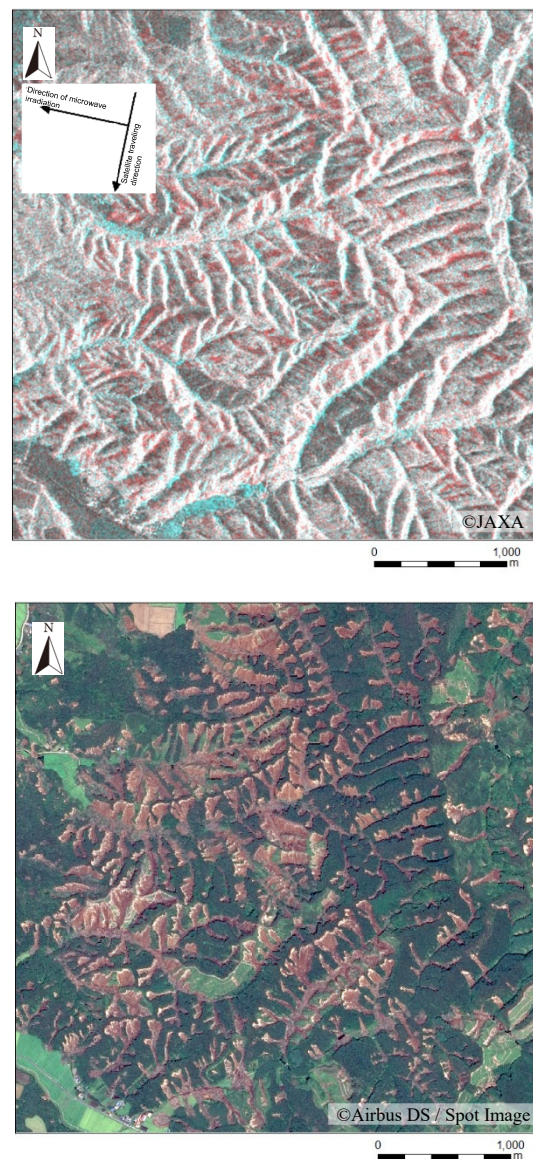


Fig.-2.3.3 Intensity difference SAR image (top) and optical image (bottom)
(Atsuma Town, Mukawa Town, Hokkaido Prefecture)

3.3 How to display and view intensity difference SAR images

To display intensity difference SAR images when carrying out the image interpretation survey of sediment disasters, it is considered that use of the scale shown in Table-2.3.2 is appropriate.

First, the images are displayed in scale of about 1:50,000, and rough survey is carried out that have a bird's eye view of the entire intensity difference SAR image. In the rough survey, whether there are changes in red, cyan, etc. is checked, and the range where detailed image interpretation will be implemented is set as shown on the left in Fig.-2.3.4.

Next, detailed survey is carried out by displaying the image in scale of about 1:25,000. As a rule of thumb, check whether there are changes for each valley, and check whether there is the range of cyan that appears when outflow of sediment occurred to the valley outlet or plain area such as a valley bottom plain and whether there is the range of red that may appear on a slope that has turned into bare land due to failure in the upstream side of such plain area (Fig.-2.3.4, center). It is desirable that image interpretation be done, being aware of the continuity of phenomena, such as estimating a slope failure in the invisible range from the changes shown in cyan in the plain area.

Lastly, an intensity difference SAR image is displayed in scale of about 1:10,000, and judgment is made on each slope unit (Fig.-2.3.4, right). It is recommended to use a judgment method to be described later.

Table-2.3.2 Rule of thumb of scale when displaying intensity difference SAR images

Survey stage	Scale
Rough survey (Bird's eye view of the entire image)	1:50,000
Detailed survey (Image interpretation of each valley)	1:25,000
Judgment (Image interpretation of each slope)	1:10,000

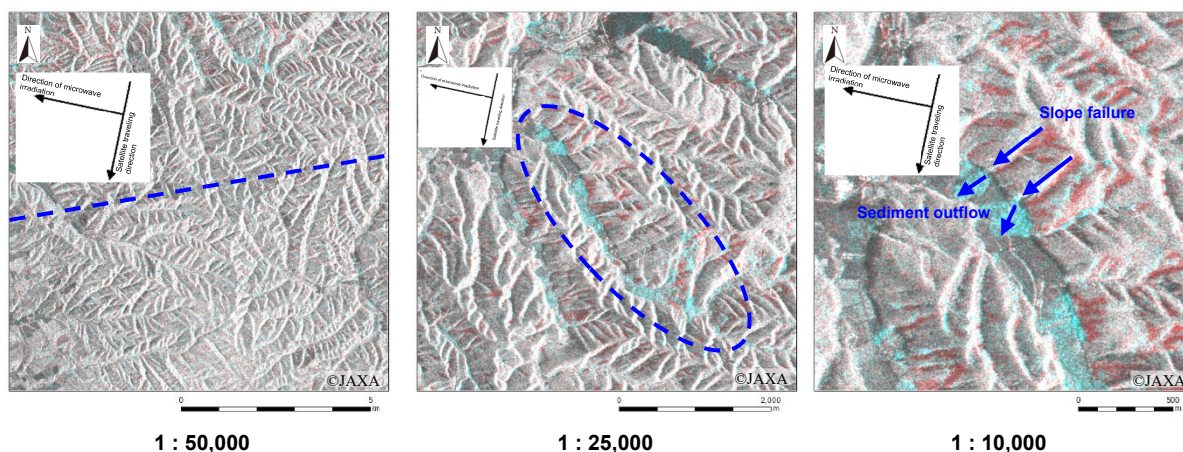


Fig.-2.3.4 Intensity difference SAR images displayed in each scale and how to view the images (Atsuma Town, Hokkaido Prefecture)

3.4 Flow of the image interpretation survey of sediment disasters by means of intensity difference SAR images

It is desirable to proceed with the image interpretation survey of sediment disasters by means of intensity difference SAR images by taking Steps 1 to 3 below.

In Step 1, judgment is made based on the minimum necessary items by placing emphasis on quick reportability of the survey (Fig.-2.3.5). First, check the changes around the slopes in the intensity difference SAR image, and when there is a change in red or pair-like change in red/cyan, compare the single-polarized SAR images before and after the disaster by visual checks. If the single-polarized SAR image after the disaster appears to be dented as though concave topography has been formed, the possibility of occurrence of a slope failure is suspected. Also, if changes in cyan are dominant, the single-polarized SAR image should be checked visually in the same manner, and if changes such as those with swollen topography can be identified, sediment may have been deposited by a failure. If changes in red or cyan cannot be identified on the intensity difference SAR image, or if changes in topography (dents and projections) cannot be identified from comparison of the single-polarized SAR images before and after the disaster, it is determined that judgment by means of intensity difference SAR images is difficult.

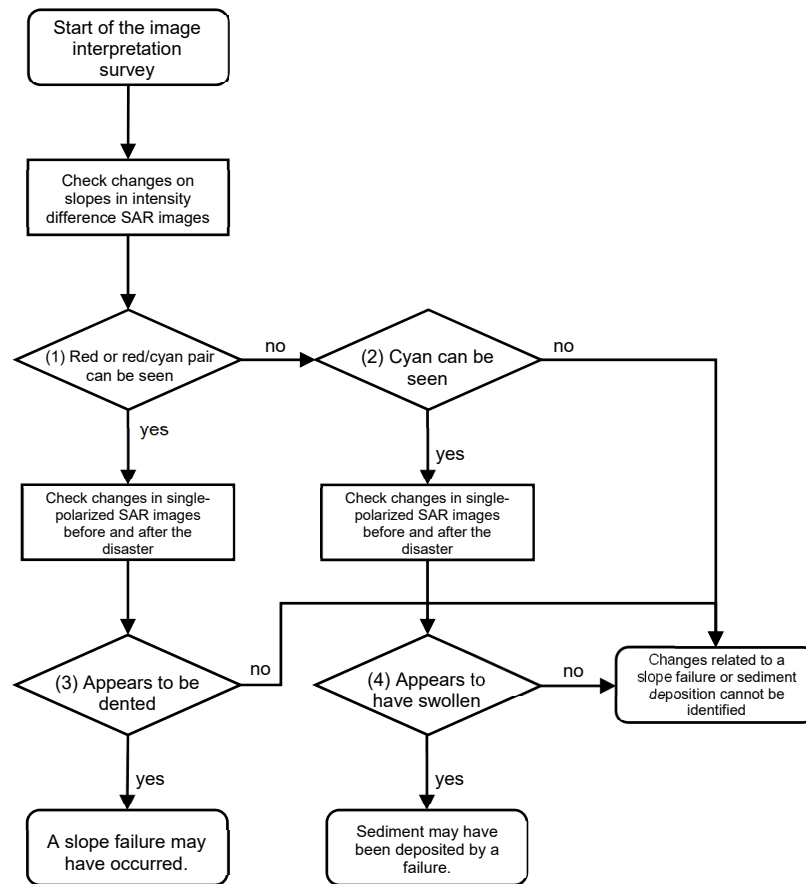


Fig.-2.3.5 Flow of the image interpretation survey of sediment disasters by means of intensity difference SAR images (Step 1)

In Step 2, the place extracted in Step 1 is evaluated as to its certainty based on the materials other than the SAR images (Fig.-2.3.6). In the case of initial response to a disaster having high emergency, this step may be omitted, but if there are few places to be extracted, implementation of this step is desirable.

In Step 1, when falling under "A slope failure may have occurred.", check that the place is an inclined land based on a topographical map. Its standard is that a slope of 20° or more in gradient should be included, and the like. Next, by referring to the topographical map and optical image (satellite photo, aerial photo, etc.) before the disaster, check that there is a low possibility of artificial modification of the slope in question, and that it was a forest before the disaster. If all the conditions stated above are met, it is determined that "It is highly likely that a slope failure has occurred."

Also, when it has been determined that "Sediment may have been deposited by a failure.", in the same manner, check that the place is a flatland based on the topographical map. We consider that, as for the standard for determining that the place is a flatland, determination from the topography such as valley outlet or valley bottom plain and the land utilization such as residential land or farmland would suffice. After that, by referring to the topographical map and optical image before the disaster,

check that there is a low possibility of artificial modification in the applicable range, and that the place is adjacent to changes in red. If all the conditions stated above are met, it is determined that "It is highly likely that sediment has been deposited by a failure."

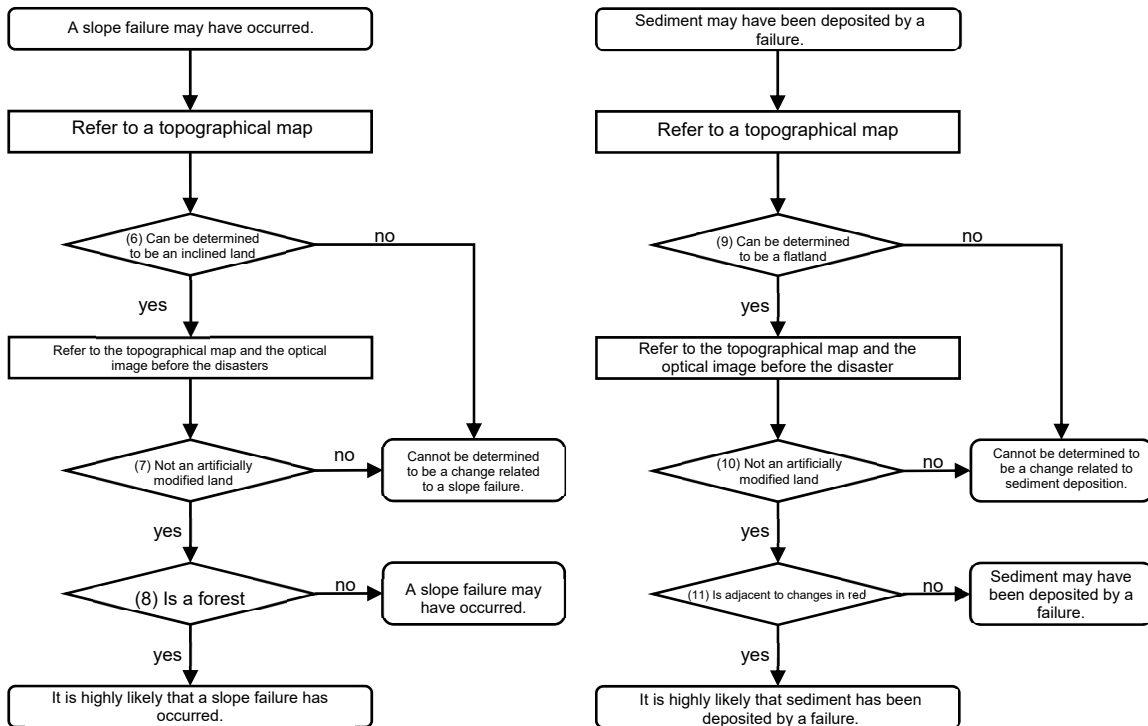


Fig.-2.3.6 Flow of the image interpretation survey of sediment disasters by means of intensity difference SAR images (Step 2)

In Step 3, the possibility of channel blockage formation is checked for all the places falling under "A slope failure may have occurred." in Step 1 (Fig.-2.3.7). In consideration of emergency of identifying the place of channel blockage, in the same manner as in Step 1, it is desirable to carry out mandatory checks and use the results for an initial report.

From the intensity difference SAR images, check whether changes in cyan can be seen in the channel, and whether ranges in red can be seen in the upstream side of the channel, and when falling under both of these, refer to the topographical map and the optical images before the disaster, to ensure that such changes or ranges are not existing dams, reservoirs, etc. that have been misinterpreted. If all the conditions stated above are met, it is determined that "It is highly likely that channel blockage may have been formed." Also, when SAR images that were observed in the initial response period are used, it is expected that the scale of inundation is small as a result of channel blockage, and therefore it is desirable that monitoring and additional survey be carried out for places in which it has been determined that "Channel blockage may have been formed." as well.

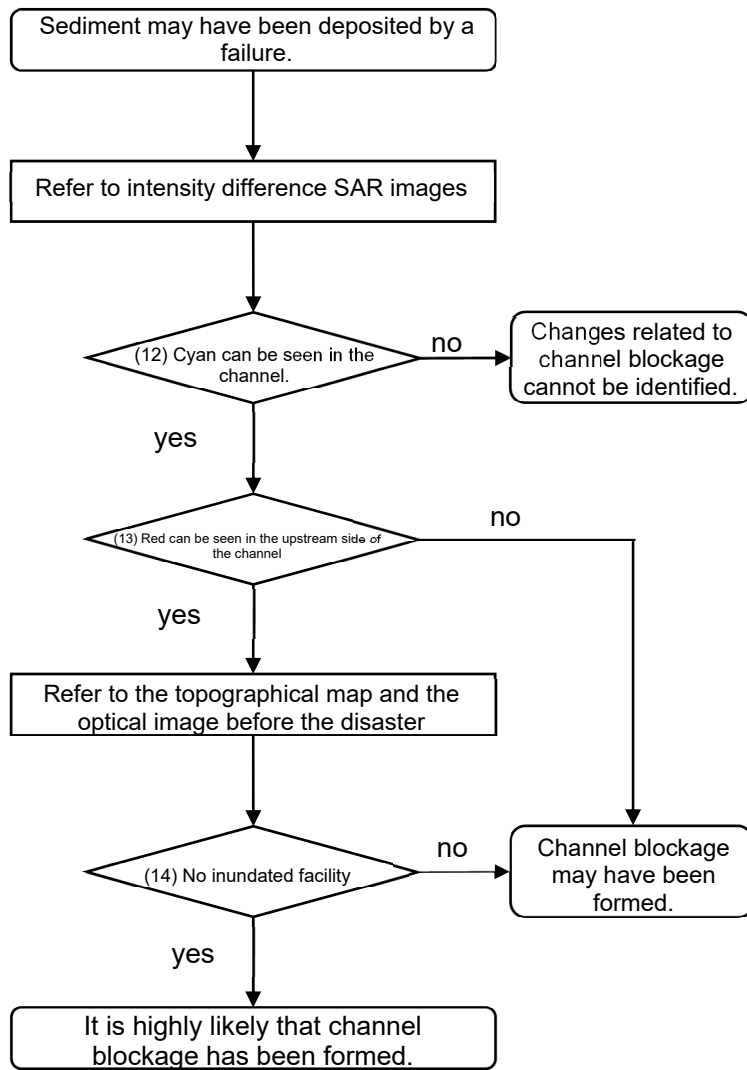


Fig.-2.3.7 Viewpoints of whether channel blockage has been formed by means of intensity difference SAR images (Step 3)

3.5 Checklist of the image interpretation survey of sediment disasters by means of intensity difference SAR images

In the image interpretation survey of sediment disasters by means of intensity difference SAR images, since the evaluation viewpoints, experiences, etc. of the surveyor may affect the results of evaluation, it is necessary to secure a certain level of accuracy as the results of generalized image interpretation survey of sediment disasters. Therefore, it is recommended to utilize the Checklist of the image interpretation survey of sediment disasters by means of intensity difference SAR images (hereinafter called the "Checklist") shown in Fig.-2.3.8. For each item in the Checklist, input the information and evaluation shown in Table-2.3.3.

In actual practice, the survey time will be prolonged if the judgment results are obtained by applying the Checklist for all the slope failures that occurred frequently like those in the 2018 Hokkaido Eastern Iburi Earthquake, and therefore it is desirable that, individual judgment be made by using the Checklist for representative places, and then comprehensive judgment be made based on the results of such judgment.

Image Interpretation Survey of Sediment Disasters by Means of Intensity Difference SAR Images Checklist

No.

ID	Location	Latitude			
		Longitude			
Intensity difference SAR image		Single-polarized SAR image (before disaster)		Single-polarized SAR image (after disaster)	
Topographical map		Optical image before disaster			
Step	Images, etc. to be referred to	Range to be checked	Check item	Judgment criteria	Evaluation (O*)
1	Intensity difference SAR image	Coloring range of intensity difference SAR image	Dominant color	(1) Red or red/cyan pairs can be seen	
				(2) Cyan can be seen	
	Single-polarized SAR image	Changes in single-polarized SAR image before and after the disaster	Shape change	(3) Appears to be dented	
				(4) Appears to have swollen	
	Intensity difference SAR image	Coloring range of intensity difference SAR image	Clarity	(5) Is clear	
(1),(3): O => 2 (failure) (2), (4): O => 2 (deposition)					
2 (failure)	Topographical map	Topography	Slope gradient	(6) Is an inclined land	
	Topographical map Optical image before disaster	Surroundings	Land cover	(7) Not an artificially modified land	
	Topographical map Optical image before disaster	Surroundings	Land cover	(8) Is a forest	
2 (deposition)	Topographical map	Topography	Slope gradient	(9) Is a flat land	
	Topographical map Optical image before disaster	Surroundings	Land cover	(10) Not an artificially modified land	
	Topographical map Optical image before disaster	Surroundings	Positional relationship	(11) Is adjacent to changes in red	
3	Intensity difference SAR image	In the channel	Dominant color	(12) Cyan can be seen	
		Upstream side of the channel		(13) Red can be seen	
	Topographical map Optical image before disaster	Upstream side of the channel	Inundated facility	(14) No inundated facility	
Judgment results		a. Occurrence of a slope failure May have occurred / Changes cannot be verified b. Sediment deposition caused by a failure May have occurred / Changes cannot be verified c. Formation of channel blockage May have occurred / Changes cannot be verified d. Image interpretation cannot be made sufficiently from SAR images			

Fig.-2.3.8 Checklist of the image interpretation survey of sediment disasters by means of intensity difference SAR images

Table-2.3.3 Changes in color and backscatter intensity on intensity difference SAR images

Item	Input	Contents to be input
No	Arbitrary	Assign an arbitrary number for handling with the results of image interpretation survey.
ID	Arbitrary	Assign an arbitrary code for managing the place of image interpretation survey.
Location	Arbitrary	Enter the address of the place of image interpretation survey.
Latitude/Longitude	Mandatory	Input the latitude and longitude of the place of image interpretation survey.
Intensity difference SAR image	Mandatory	Paste the intensity difference SAR image of the place of image interpretation survey.
Single-polarized SAR image (before disaster)	Mandatory	Paste the single-polarized SAR image (before disaster) of the place of image interpretation survey.
Single-polarized SAR image (after disaster)	Mandatory	Paste the single-polarized SAR image (after disaster) of the place of image interpretation survey.
Topographical map	Arbitrary	Paste the topographical map of the place of image interpretation survey.
Optical image before disaster	Arbitrary	Paste the optical image before disaster of the place of image interpretation survey.
Step 1	Mandatory	Carry out evaluation according to Fig.-2.3.5. Note that for (5), carry out relative evaluation in the range of survey, arbitrarily.
Step 2 (failure/deposition)	Arbitrary	Carry out evaluation according to Fig.-2.3.6.
Step 3	Mandatory	Carry out evaluation according to Fig.-2.3.7.
Judgment results	Mandatory	Based on the results of evaluation, enter a to d so that the applicable place can be understood.

An example of utilization of flow of the image interpretation survey and the Checklist in the 2018 Hokkaido Eastern Iburi Earthquake is shown (Fig.-2.3.9).

The place of image interpretation survey on the intensity difference SAR image (the valley shown in the blue circle in Fig.-2.3.9) has changes in red in the slope part, and all the check items in Step 1 from the valley outlet to changes in cyan, etc. have been verified, and it has been determined that a slope failure may have occurred and sediment deposition by the failure may have occurred. In addition, any of the failure and deposition in Step 2 is also applicable. Therefore, it can be estimated that the occurrence of a slope failure and the deposition of sediment caused by the failure have occurred with a high degree of certainty. And in Step 3, cyan could be identified in the channel, but no changes in red can be seen in the upstream part of the channel, and therefore it has been determined that no changes can be verified concerning the formation of channel blockage.

Based on the above results of evaluation, it has been determined that there is a sufficient possibility that in the place in question, a slope failure has occurred and sediment deposition caused by the failure has occurred, but changes of the formation of channel blockage cannot be verified.

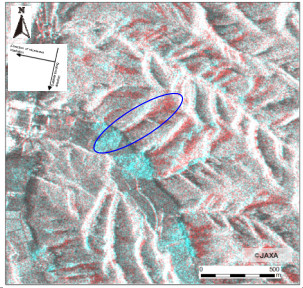
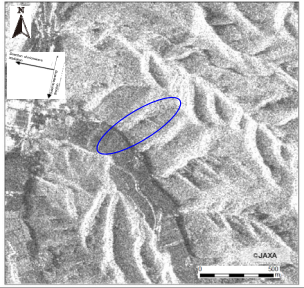
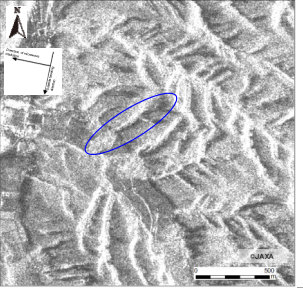
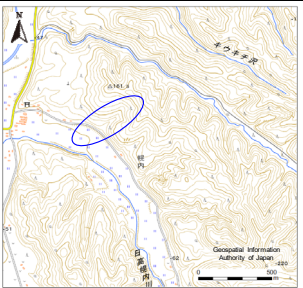
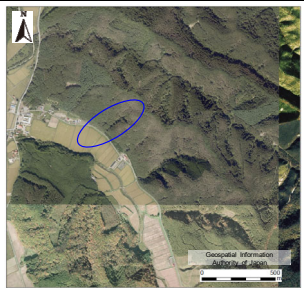
ID	Example of entry	Location	Aza Horonai, Atsuma Town, Yufutsu County, Hokkaido Prefecture		Latitude	42.753956
			Longitude	141.985929		
Intensity difference SAR image		Single-polarized SAR image (before disaster)		Single-polarized SAR image (after disaster)		
						
Topographical map		Optical image before disaster				
						
Step	Images, etc. to be referred to	Range to be checked	Check item	Judgment criteria	Evaluation (Ox)	
1	Intensity difference SAR image	Coloring range of intensity difference SAR image	Dominant color	(1) Red or red/cyan pairs can be seen	O	
	Single-polarized SAR image	Changes in single-polarized SAR image before and after the disaster	Shape change	(3) Appears to be dented (4) Appears to have swollen	O	
	Intensity difference SAR image	Coloring range of intensity difference SAR image	Clarity	(5) Is clear	O	
(1),(3): O => 2 (failure) (2), (4), O => 2 (deposition)						
2 (failure)	Topographical map	Topography	Slope gradient	(6) Is an inclined land	O	
	Topographical map Optical image before disaster	Surroundings	Land cover	(7) Not an artificially modified land	O	
	Topographical map Optical image before disaster	Surroundings	Land cover	(8) Is a forest	O	
2 (deposition)	Topographical map	Topography	Slope gradient	(9) Is a flat land	O	
	Topographical map Optical image before disaster	Surroundings	Land cover	(10) Not an artificially modified land	O	
	Topographical map Optical image before disaster	Surroundings	Positional relationship	(11) Is adjacent to changes in red	O	
3	Intensity difference SAR image	In the channel	Dominant color	(12) Cyan can be seen	O	
		Upstream side of the channel		(13) Red can be seen	x	
	Topographical map Optical image before disaster	Upstream side of the channel	Inundated facility	(14) No inundated facility	O	
Judgment results		a. Occurrence of a slope failure <i>May have occurred / Changes cannot be verified</i> b. Sediment deposition caused by a failure <i>May have occurred / Changes cannot be verified</i> c. Formation of channel blockage <i>May have occurred / Changes cannot be verified</i> d. Image interpretation cannot be made sufficiently from SAR images				

Fig.-2.3.9 Checklist of the image interpretation survey of sediment disasters by means of intensity difference SAR images (example of entry)

4. Application of the image interpretation survey of sediment disasters by means of SAR images

4.1 Efficient method of image interpretation survey

4.1.1 Utilization of the display functions of GIS software, etc.

"Image permeation display" and "image swipe display" with which GIS software is often provided as standard are the functions for increasing the efficiency of image interpretation survey when referring to multiple image data and when handling both ground range images and ortho images.

4.1.2 Utilization of GIS data

Collect GIS data such as those of administrative boundaries, rivers, roads, and sediment disaster warning areas, and use them as a reference during image interpretation. At this time, since the ground range images and GIS data are not overlapped in the same place, attention should be paid to this during image interpretation, and the position should be specified by referring to a topographical map, etc.

4.1.3 Utilization of ground range images

Use SAR images in the ground range in which the distance from the target object has been projected by SAR to the ground surface (Fig.-2.4.1). By performing ortho processing (orthographic projection) of the image, it can be overlapped accurately with GIS data such as topography or administrative boundaries, but as a result of distortion of the image, the visibility of a failure area, channel, etc. decreases. On the other hand, since a ground object is photographed as an image like that of an oblique photo, its intuitive interpretation can be performed easily. Moreover, since ortho processing takes a lot of time, when speedy image interpretation is required, the use of ground range images is recommended that provides data quickly.

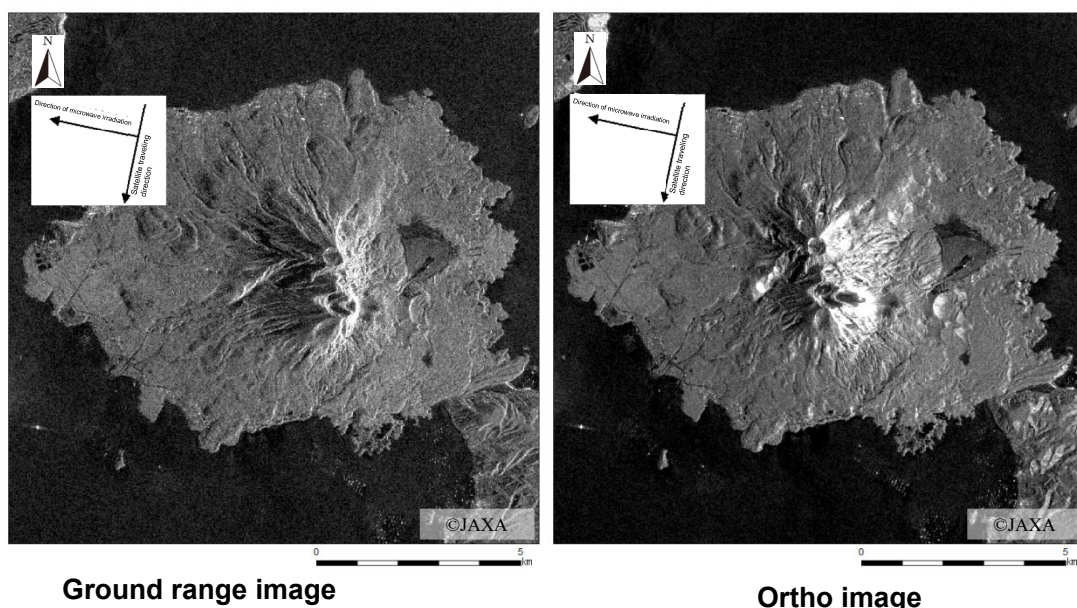


Fig.-2.4.1 Comparison of ground range image and ortho image (Sakurajima, Kagoshima City, Kagoshima Prefecture)

4.1.4 Image erecting

Since a SAR image has dependency on the direction, image interpretation is performed by erecting the image, visibility increases. When erecting a SAR image, the stereoscopic feeling of the topography is emphasized by making the direction of microwave irradiation (direction in which the topography falls down due to layover) face upward (Fig.-2.4.2).

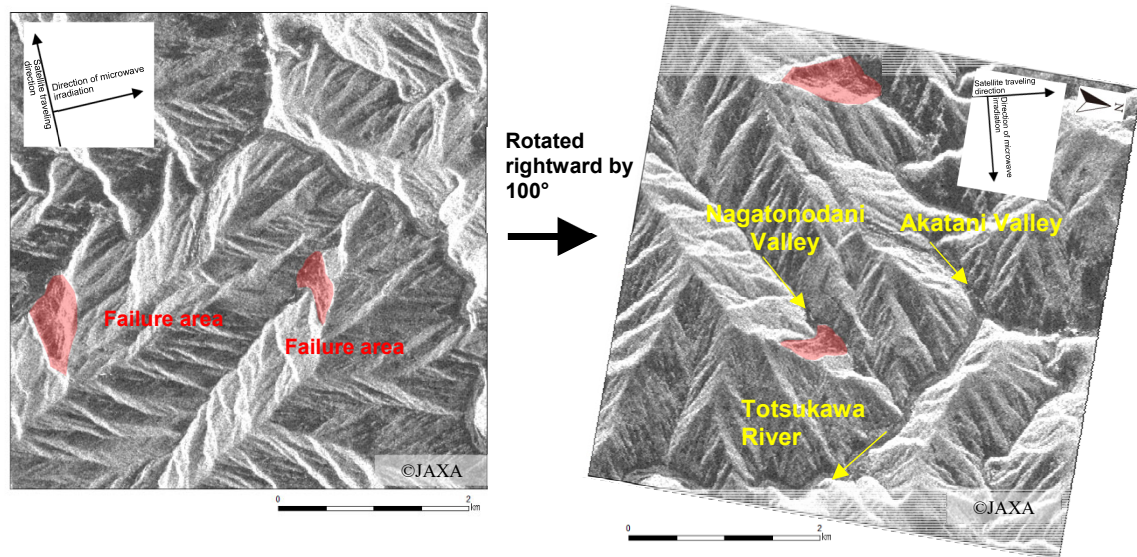


Fig.-2.4.2 Visibility when a SAR image has been erected
(Gojo City/Totsukawa Village, Nara Prefecture)

4.2 Method of image interpretation survey that increases the reliability of results

4.2.1 Filtering of SAR images

SAR images contain spot-like noise called "speckle noise," and this noise becomes a factor of decreasing the visibility of the image and the accuracy of synthetic processing of the image, etc. For this reason, it is desirable to perform filtering of the SAR images to be used for image interpretation survey. As a general rule of thumb, filtering is often used in which the average and median of 3×3 pixels are obtained.

Fig.-2.4.3 shows intensity difference SAR images with which a comparison is made between with filtering and without filtering. Even if filtering is done, changes in red or cyan are not subject to the effects of filtering, and visibility increases as a result of reduction of only the effects of the spots in the form of black and white in the SAR image. Note that when intensity difference SAR images, etc. are to be generated, single-polarized SAR images before color synthesis processing need to be filtered.

Note that the time required for filtering varies with the size of the SAR image and the type of the filter, it takes about several minutes to perform processing with which ordinary software is provided as standard.

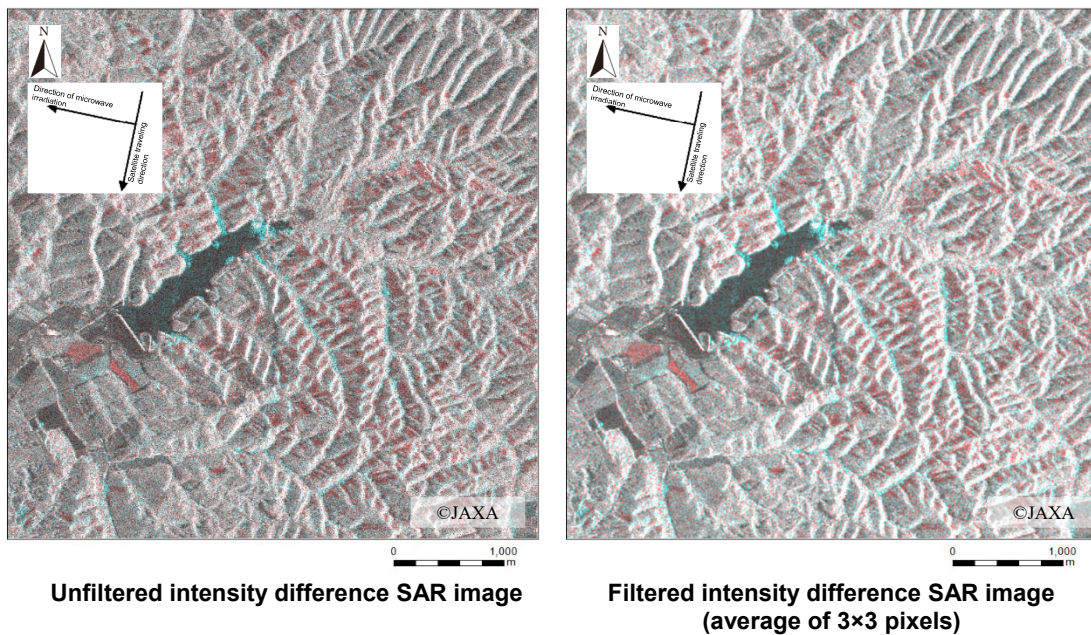


Fig.-2.4.3 Comparison of intensity difference SAR images between filtered and unfiltered ones (Abira Town, Hokkaido Prefecture)

4.2.2 Additional survey of invisible ranges

As will be described later in "Part 2, 5.2 Orientation of a slope relative to the direction of microwave irradiation", the image interpretation survey of sediment disasters by means of SAR images is subject to deviation in detectability due to the relationships between the direction of microwave irradiation and the slope direction, with many invisible ranges occurring on slopes in specific directions. For this reason, it is desirable to wait for the opportunity of satellite observation and obtain SAR images produced by irradiating microwaves from the reverse direction, and carry out image interpretation survey of sediment disasters additionally.

5. Precautions for the techniques for the image interpretation survey of sediment disasters by means of SAR images

5.1 Effects of artificial modification

In a mountainous region where the occurrence of a slope failure is expected, deforested area or a quarry shows changes in the backscatter intensity that are similar to those of a slope failure (Fig.-2.5.1). When a forest is lost by deforestation, volume scattering that was dominant before the disaster disappears, and consequently the backscatter also decreases greatly, which appears on the intensity difference images as changes in red or of red-cyan pairs (Fig.-2.5.2). Also, similar changes appear as a result of the retreat of a slope caused by quarrying changing the position of the scattering surface, or as a result of a change in local incidence angle caused by a change in the slope gradient (Fig.-2.5.3).

These are difficult to be distinguished from changes in the backscatter intensity of a slope failure in image interpretation survey by visual checks, and the following can be considered as the measures for avoiding erroneous image interpretation.

- (1) Check whether there are changes in cyan caused by outflow of sediment to a plain area, etc.
- (2) Use the most recent archive SAR images within the available range.
- (3) Make judgment based on the shape of changes such as artificial rectangular shape, regularity, etc.
- (4) Check the effects of artificial modification based on the optical image before the disaster.

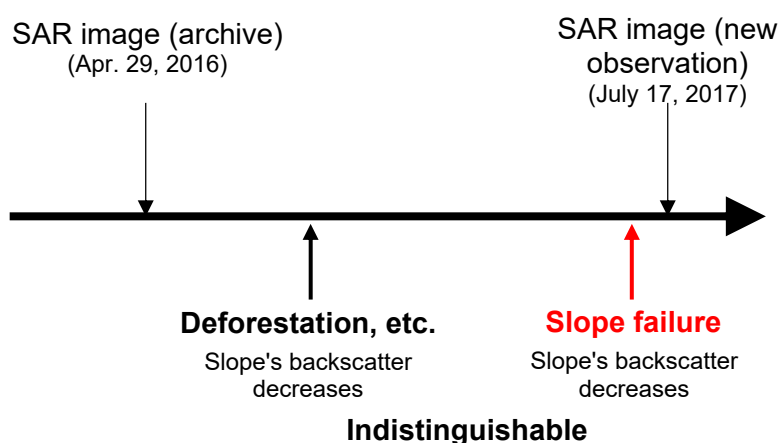


Fig.-2.5.1 Case where distinction between slope failure and artificial modification becomes difficult in intensity difference SAR images

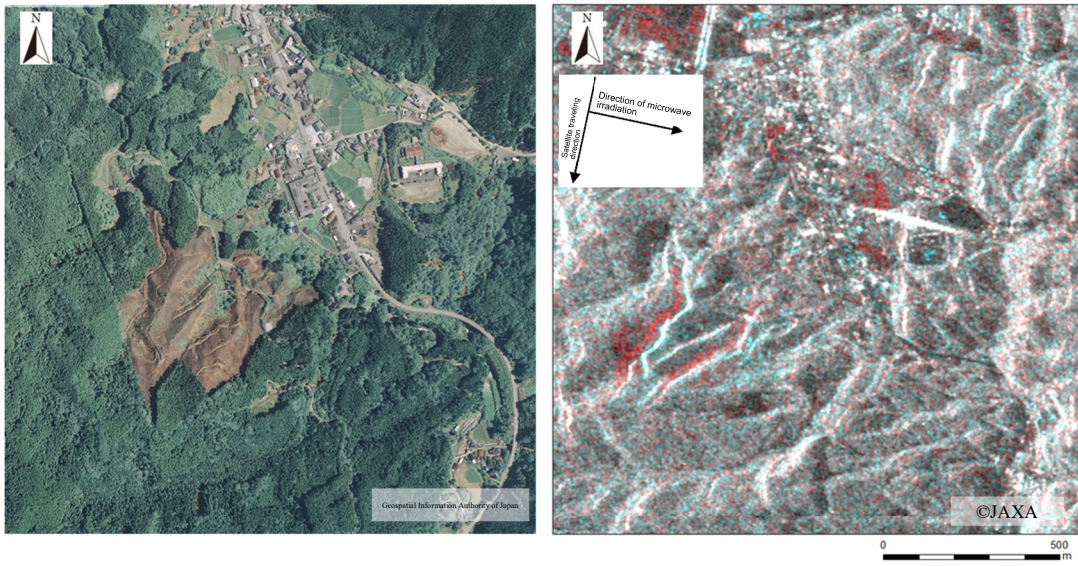


Fig.-2.5.2 Example in which changes in backscatter caused by deforestation appeared (Toho Village, Fukuoka Prefecture)

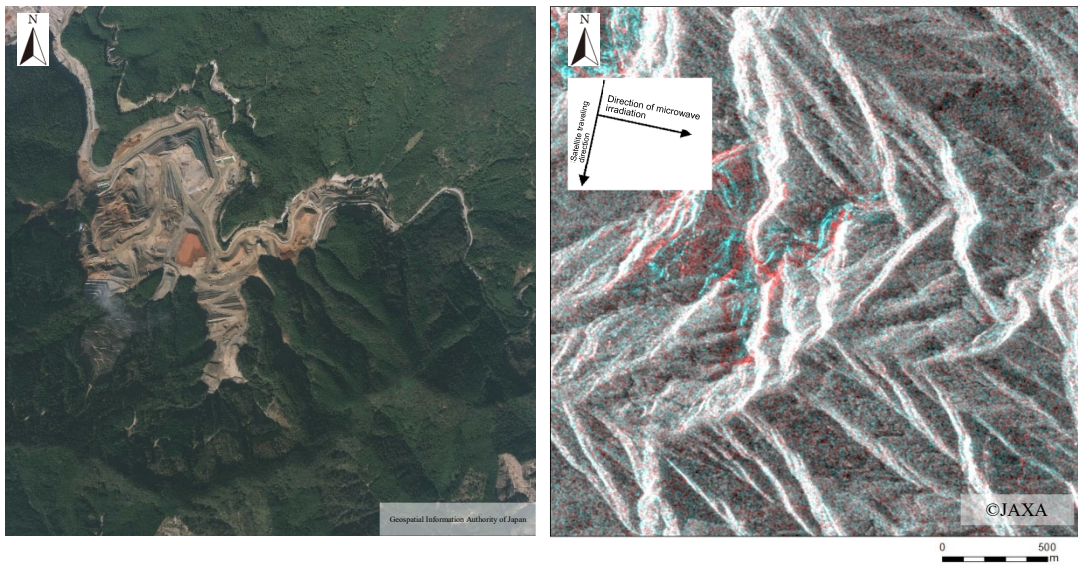


Fig.-2.5.3 Example in which changes in backscatter caused by quarrying appeared (Asakura City/Toho Village, Fukuoka Prefecture)

5.2 Orientation of a slope relative to the direction of microwave irradiation

SAR images are projected by being strongly affected by the geometrical conditions due to the irradiation angle of microwaves, etc., and an invisible range is generated by the effects of the geometric image modulation described in "Part 1, 2.3 Precautions for SAR images."

Fig.-2.5.4, left shows the invisible range derived by the geometrical calculations of the irradiation angle of microwaves with a topographical model (10 m numerical value altitude model). In places where many slope failures occurred with various slope orientations, when the aerial photo taken after the disaster (Fig.-2.5.4, center) is compared with the intensity difference SAR image (Fig.-2.5.4, right), it can be seen that visibility on the intensity difference SAR image varies greatly with the slope orientation, and it is estimated that this effect is related to the accuracy of the image interpretation survey.

Namely, if the off nadir angle set as the recommended condition in this material is around 30° to 45° , the slope facing the direction of microwave irradiation (west-facing slope in Fig.-2.5.4) is the invisible range caused by layover, and therefore sufficient results of survey by image interpretation cannot be obtained. As shown in Fig.-2.5.5, even in the case of a large-scale slope failure of about $76,600 \text{ m}^2$ in area, image interpretation becomes difficult when being strongly subjected to the effect of layover at the slope orientation facing the direction of microwave irradiation (east-facing slope in Fig.-2.5.5).

Since this effect cannot be reduced when handling SAR images, practically attention needs to be paid to the following points.

(1) Make judgment after checking changes in cyan on a flatland, etc. that is unlikely to be affected by layover.

(2) Implement image interpretation survey and handle the results of survey by bearing in mind the occurrence of an invisible range.



Fig.-2.5.4 Comparison of visibility in invisible ranges (Higashihiroshima City/Yasuura Town, Hiroshima Prefecture)

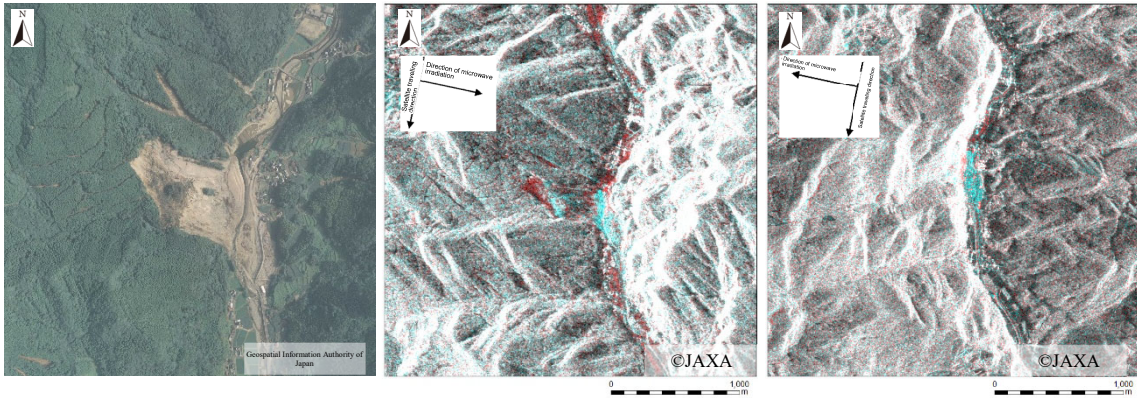


Fig.-2.5.5 Comparison of visibility depending on the direction of microwave irradiation
(Hita City, Oita Prefecture)

Center: direction of microwave irradiation [east → west]

Right: direction of microwave irradiation [west → east]

Part 3 Results of application of the image interpretation survey of sediment disasters by means of intensity difference SAR images

1. Time required for the image interpretation survey of sediment disasters by means of intensity difference SAR images

Table-3.1.1 shows a rule of thumb for the time required for the image interpretation survey of sediment disasters by means of intensity difference SAR images by the confirmation of response to 7 cases of disasters. In the disasters caused by rainfall, the time was about 35 hours from the occurrence of the disaster (announcement of sediment disaster warning information), and in the disasters caused by an earthquake, it was about 15 hours from the occurrence of the earthquake. Although some parts greatly depend on the observation by the satellite, it takes about 7 hours to carry out the image interpretation survey of sediment disasters after observation by means of SAR.

Based on the above results, it can be said that the image interpretation survey of sediment disasters by means of intensity difference SAR images is a method that enables the results of survey to be obtained in about 0.5 to 1.5 days from the occurrence of danger of the occurrence of sediment disasters.

Table-3.1.1 Time required for the image interpretation survey of sediment disasters by means of intensity difference SAR images

Disaster name	Required time [h]		
	Occurrence of disaster - SAR observation	SAR observation - Image interpretation survey	Occurrence of disaster - Image interpretation survey
2017 Southern Nagano Earthquake	4.9	8.7	13.5
Torrential Rainfall in Shimane Prefecture in July 2017	11.9	7.1	19.1
Northern Kyushu Torrential Rainfall in July 2017	46.7	7.1	53.8
2017 Typhoon No. 21	19.5	7.3	26.8
2018 Northern Osaka Earthquake	16.0	9.2	25.2
Torrential Rainfall in July 2018	33.9	7.9	41.8
2018 Hokkaido Eastern Iburi Earthquake	8.6	3.8	12.4
Average (all)	20.2	7.3	27.5
Average (rainfall disaster)	28.0	7.4	35.4
Average (earthquake disaster)	9.8	7.2	17.0
Median (all)	16.0	7.3	25.2
Median (rainfall disaster)	26.7	7.2	34.3
Median (earthquake disaster)	8.6	8.7	13.5

2. Accuracy of the image interpretation survey of sediment disasters by means of intensity difference SAR images

2.1 Conditions of verification of accuracy

For the 4 cases of sediment disasters that occurred on a large-scale and in a wide area, "2016 Kumamoto Earthquake," "Northern Kyushu Torrential Rainfall in July 2017," "Torrential Rainfall in July 2018" and "2018 Hokkaido Eastern Iburi Earthquake," the accuracy of the image interpretation survey of sediment disasters by means of intensity difference SAR images was checked.

The verification of accuracy was made for the places in SAR images excluding the invisible ranges, carrying out evaluation by using the percentage of the places where the occurrence of a sediment disaster is determined to have a high probability from the intensity difference SAR images (hereinafter called the "detection target") in the places where a sediment disaster occurred selected from the results of image interpretation of aerial photos, etc. taken after the disaster (hereinafter called the "verification target") as the detection rate [%].

The verification target was selected so that the targets are roughly uniform in relation to the criteria shown in Fig.-3.2.1: "disaster trigger factor," "area (area in orthographic projection)," "slope gradient," "slope direction (clockwise angle with the north set to 0°)." Also, as for the detection target, the number of cases was used that were determined as "A slope failure may have occurred." or "Sediment may have been deposited by a failure." from the evaluation in Step 1 in "Part 2, 3.4 Flow of the image interpretation survey of sediment disasters by means of intensity difference SAR images", which is equivalent to the accuracy during the initial disaster investigation. The detection rate was checked for each of the items: "area," "slope gradient," "slope direction," "local incidence angle," and "relative direction angle (angle expressed by $\pm 180^\circ$ with the direction facing the direction of microwave irradiation being set to 0°)."

Note that this verification gives the results of using the places of a scale or shape with which it can be judged that a sediment disaster could have surely occurred as the verification target, and small-scale failures of which image interpretation cannot be made from aerial photos, etc. and failures in the shadow of a forest, etc. have not been checked due to the nature of the data used for verification.

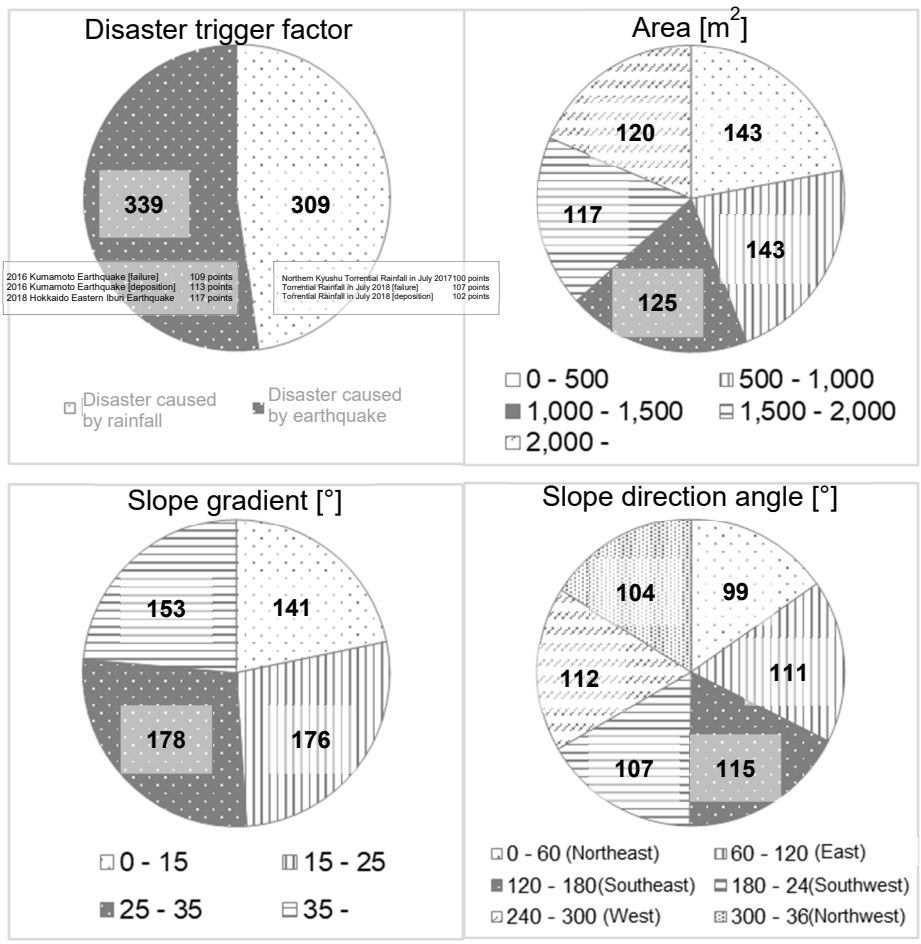


Fig.-3.2.1 Number of verification targets for each selection criterion (N = 648)

2.2 Results of verification of accuracy

The accuracy of the image interpretation survey of sediment disasters by means of intensity difference SAR images is shown below.

As shown in Fig.-3.2.2, the area and accuracy have correlations, and it can be seen that the greater the scale of changes, the higher the detection rate. When a slope failure or outflow/deposition of sediment of 2000 m² or more in area has occurred, it can be detected with a probability of about 70%.

The slope gradient and slope direction are not the factors that directly affect the detection rate (Fig.-3.2.3, Fig.-3.2.4). On the other hand, the local incidence angle and relative direction angle greatly affects the detection rate. As for the local incidence angle shown in Fig.-3.2.5, as the angle increases, the detection rate improves, and the detection rate reaches its maximum, being about 50%, when the angle is 45 to 60°. When the angle reaches to a higher value of 75 to 90°, the tendency of the detection rate decrease can be seen, but it is a result of a small number of verifications, and such tendency is uncertain. By referring to "Reference material 2. Accuracy of the image interpretation survey of sediment disasters by means of intensity difference SAR images in each disaster," unevenness can be seen in the relationships between local incidence angle and detection rate in each disaster, but in any of the disasters, the detection rate is very low when the local incidence angle is extremely small or extremely large. Also, as for the relative direction angle in Fig.-3.2.6, the detection rate has a tendency such that it reaches the lowest value, being about 15 to 25% when the angle is 0 to ±60°, and the detection rate becomes higher, being about 50 to 60% when the angle is ±120 to ±180°. It is considered that this is due to the fact that, as described in "Part 2, 5.2 Orientation of a slope relative to the direction of microwave irradiation," since the slope facing the direction of microwave irradiation (slope having a small relative direction angle) is an invisible range caused by the effect of layover, the detection rate becomes extremely low.

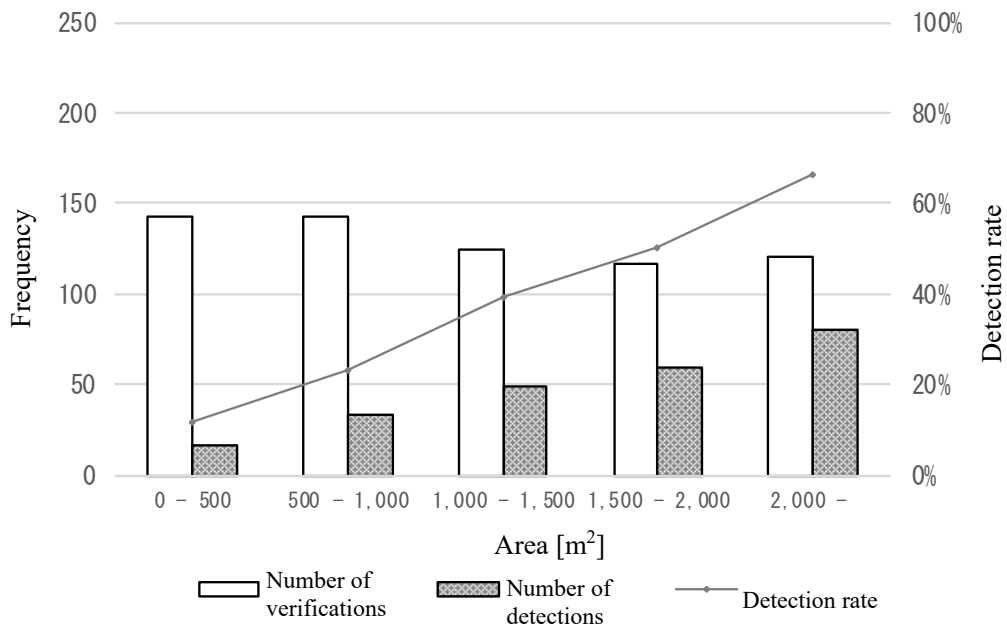


Fig.-3.2.2 Detection rate in the image interpretation survey of sediment disasters by means of intensity difference SAR images (area)

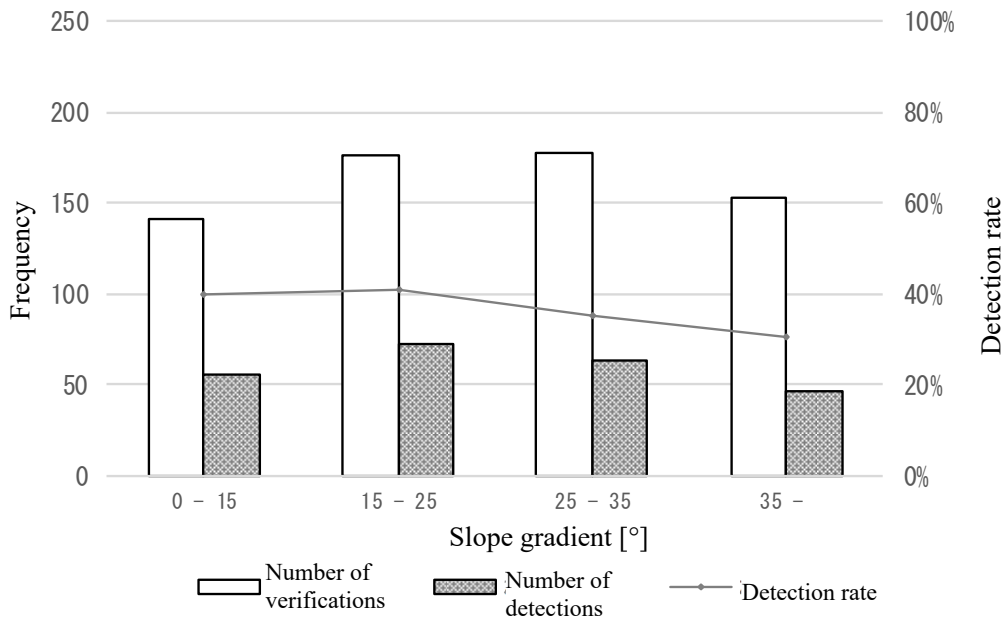


Fig.-3.2.3 Detection rate in the image interpretation survey of sediment disasters by means of intensity difference SAR images (slope gradient)

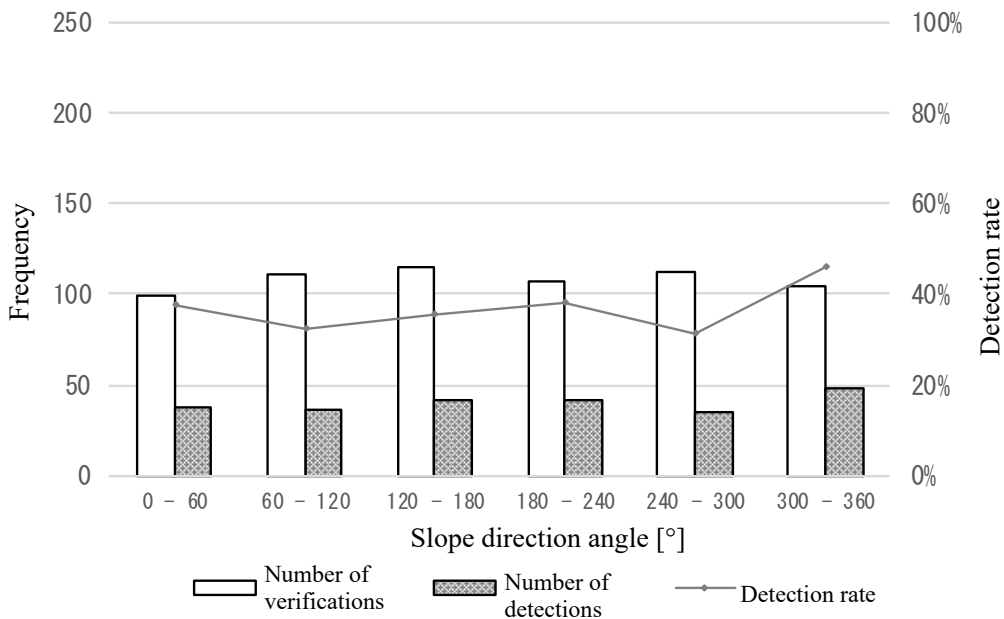


Fig.-3.2.4 Detection rate in the image interpretation survey of sediment disasters by means of intensity difference SAR images (slope direction angle)

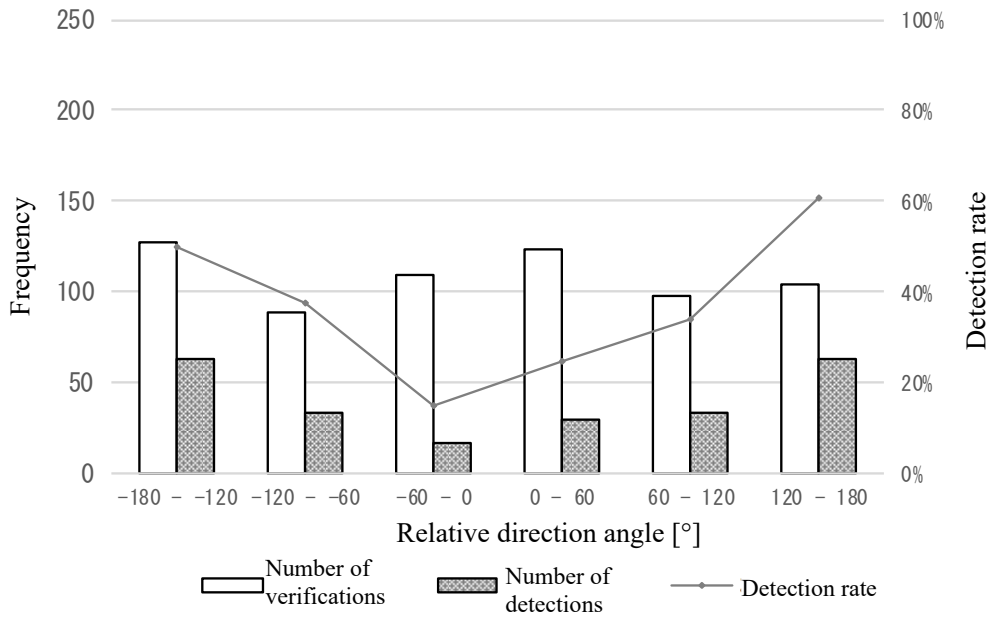


Fig.-3.2.5 Detection rate in the image interpretation survey of sediment disasters by means of intensity difference SAR images (relative direction angle)

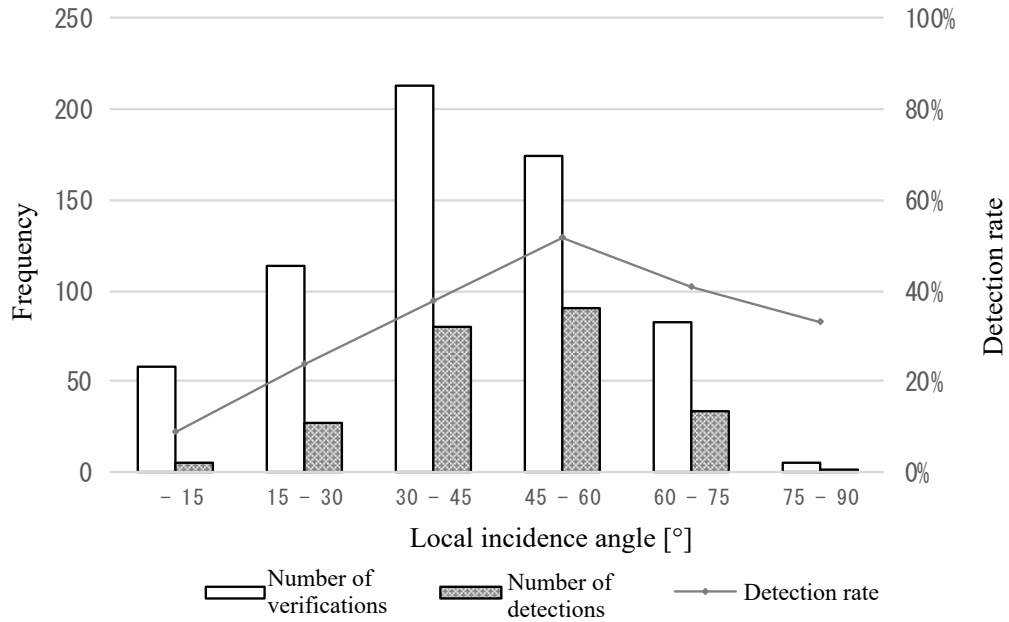


Fig.-3.2.6 Detection rate in the image interpretation survey of sediment disasters by means of intensity difference SAR images (local incidence angle)

References

- 1) Masaki Mizuno, Joko Kamiyama, Masafumi Ekawa, Takumi Satou, Junichi Kanbara, Shin-ichiro Hayashi (2013): Method of emergency search for the location of landslide dams using high-resolution single-polarization SAR image interpretation, Technical Note of National Institute for Land and Infrastructure Management No. 760
- 2) Masaki Mizuno, Joko Kamiyama, Masafumi Ekawa, Takumi Satou, Junichi Kanbara (2014): Method of emergency search for the location of landslide dams and collapses using high-resolution dual-polarization SAR image interpretation, Technical Note of National Institute for Land and Infrastructure Management No. 791
- 3) Yamato Suzuki, Masayuki Matsuda, Yasuhiro Nomura, Hiroaki Nakaya (2019): Application of Sediment Disaster Survey Method by Difference of Backscattering Intensity over SAR Images, Civil Engineering Journal, Vol. 61, No. 12, pp.16-19
- 4) Kumiko Yamashita, Joko Kamiyama, Yamato Suzuki, Tomoyuki Noro, Jun Sugimoto, Takashi Shibayama, Toshiaki Udono (2019): Validation of landslides detection capability using multi-temporal SAR images: A case study on the heavy rainfall in northern Kyushu in July, 2017, Journal of the Japan Society of Erosion Control Engineering, Vol. 71, No. 6, pp. 21-27
- 5) (National Research and Development Agency) Japan Aerospace Exploration Agency (2018): Satellite for Disaster Monitoring from Space - Land Observing Satellite No. 2 "Daichi 2" Disaster Case Collection 2014 to 2017 -
- 6) (National Research and Development Agency) Japan Aerospace Exploration Agency/Ministry of Land, Infrastructure, Transport and Tourism (2018): Guide Book for Artificial Satellite Utilization during Disasters - Sediment Disaster Edition http://www.mlit.go.jp/river/sabo/satellite/manual_180327.pdf
- 7) Kazuo Ouchi (2004): Basics of Synthetic Aperture Radar for Remote Sensing, Tokyo Denki University Press
- 8) Japan Association of Remote Sensing (2001): Graphic Explanation - Remote Sensing, Japan Association of Surveyors

Parameters of the SAR images in the text

Drawing number	Date & time of observation	Resolution [m]	Off nadir angle [°]	Polarization	Orbit direction	Direction of microwave irradiation
Fig.-1.2.1	2017/07/07	3	29.1	HH	Southbound	Satellite traveling direction, left
Fig.-1.2.2	2018/04/14	3	38.2	HH	Northbound	Satellite traveling direction, right
Fig.-1.2.3	2019/06/21	3	38.2	HH	Northbound	Satellite traveling direction, right
Fig.-1.2.4	2019/06/21	3	38.2	HH	Northbound	Satellite traveling direction, right
Fig.-1.2.5	2019/06/21	3	38.2	HH	Northbound	Satellite traveling direction, right
Fig.-1.2.7	2019/09/09	10	52.4	HH HV	Southbound	Satellite traveling direction, right
Fig.-1.2.8	2017/04/29 2017/07/07	3	29.1	HH	Southbound	Satellite traveling direction, left
Fig.-1.3.1	2017/04/29 2017/07/07	3	29.1	HH	Southbound	Satellite traveling direction, left
Fig.-1.3.2	2019/09/09	10	52.4	HH HV	Southbound	Satellite traveling direction, right
Fig.-1.3.3	2018/06/18	3	38.2	HH	Northbound	Satellite traveling direction, right
Fig.-2.3.1	2018/08/23 2018/09/06	3	32.4	HH	Southbound	Satellite traveling direction, right
Fig.-2.3.3	2018/08/23 2018/09/06	3	32.4	HH	Southbound	Satellite traveling direction, right
Fig.-2.3.4	2018/08/23 2018/09/06	3	32.4	HH	Southbound	Satellite traveling direction, right
Fig.-2.3.9	2018/08/23 2018/09/06	3	32.4	HH	Southbound	Satellite traveling direction, right
Fig.-2.4.1	2020/03/02	3	32.4	HH	Southbound	Satellite traveling direction, right
Fig.-2.4.2	2017/10/23	3	38.2	HH	Northbound	Satellite traveling direction, right
Fig.-2.4.3	2018/08/23 2018/09/06	3	32.4	HH	Southbound	Satellite traveling direction, right
Fig.-2.5.2	2017/04/29 2017/07/07	3	29.1	HH	Southbound	Satellite traveling direction, left
Fig.-2.5.3	2017/04/29 2017/07/07	3	29.1	HH	Southbound	Satellite traveling direction, left
Fig.-2.5.4	2018/03/17 2018/07/21	3	32.4	HH	Northbound	Satellite traveling direction, right
Fig.-2.5.5, Center	2017/04/29 2017/07/07	3	29.1	HH	Southbound	Satellite traveling direction, left
Fig.-2.5.5, Right	2017/06/12 2017/07/10	3	32.4	HH	Southbound	Satellite traveling direction, right

Reference material 1. Time required for the image interpretation survey of sediment disasters by means of intensity difference SAR images of each disaster

2017 Southern Nagano Earthquake

■ Conditions of/time required for image interpretation survey

Disaster factor	Date & time of disaster occurrence	Meteorological situation during disaster occurrence	Image interpretation area [km ²]	[A] Disaster occurrence - SAR observation	[B] SAR observation - Image interpretation survey	[A+B] Disaster occurrence - Image interpretation survey
Earthquake	2017/6/25 07:02	Rainy - Cloudy	About 3,500	4hours54minutes	8hours39minutes	13hours33minutes

■ Image interpretation survey timeline

Date & time	Transmitter	Receiver	Response, etc.
2017/6/25 07:02	-	-	An earthquake occurred in the southern part of Nagano Prefecture (a maximum seismic intensity of 5 upper was observed in Otaki Village and Kiso Town).
Around 09:00	MLIT Headquarters	JAXA	ALOS-2 Emergency Observation Request
Around 11:56	-	-	ALOS-2 observation
Around 17:00	JAXA	NILIM	ALOS-2 observation data was provided; started image interpretation.
20:01	JAXA	MLIT Headquarters - NILIM	Reported the results of image interpretation.
20:35	NILIM	MLIT Headquarters	Reported the findings in the results of image interpretation.
20:35	MLIT Headquarters	Chugoku Regional Development Bureau	Provided the results of image interpretation.
Starting at around 7:24 on June 26, the Regional Development Bureau started helicopter survey after waiting for the weather to get better. => No large-scale failure was identified.			

■ Parameters of the SAR images used for the image interpretation survey

	Observation date & time	Resolution [m]	Off nadir angle [°]	Polarization	Orbit direction	Direction of microwave irradiation	Number of scenes
Archive	May 28, 2017 Around 11:56	3	29.1 (U2-6)	HH	Descending (Southbound)	Traveling direction, right	2
New observation	June 25, 2017 Around 11:56						

Torrential Rainfall in Shimane Prefecture in July 2017

■ Conditions of/time required for image interpretation survey

Disaster factor	Date & time of disaster occurrence	Meteorological situation during disaster occurrence	Image interpretation area [km ²]	[A] Disaster occurrence - SAR observation	[B] SAR observation - Image interpretation survey	[A+B] Disaster occurrence - Image interpretation survey
Rainfall	2017/7/5 00:15	Rainy	About 2,000	11hours56minutes	7hours07minutes	19hours03minutes

■ Image interpretation survey timeline

Date & time	Transmitter	Receiver	Response, etc.
2017/7/5 00:15	-	-	Sediment disaster warning information was announced in Hamada City and Masuda City, Shimane Prefecture.
05:55	-	-	Special heavy rain warning was announced in Hamada City, Masuda City, Ohnan Town, and Tsumano Town, Shimane Prefecture.
Around 12:11	-	-	ALOS-2 observation
15:08	MLIT Headquarters	NILIM	ALOS-2 observation data was provided; started image interpretation.
17:51	NILIM	MLIT Headquarters	Reported the results of image interpretation (quick report).
19:03	JAXA	NILIM	Reported the results of image interpretation.
19:18	NILIM	MLIT Headquarters	Reported the findings in the results of image interpretation.
20:04	MLIT Headquarters	Chugoku Regional Development Bureau	Communicated the results of image interpretation.

A

B

■ Parameters of the SAR images used for the image interpretation survey

	Observation date & time	Resolution [m]	Off nadir angle [°]	Polarization	Orbit direction	Direction of microwave irradiation	Number of scenes
Archive	March 29, 2017 Around 12:11	3	38.6 (U2-9)	HH	Descending (Southbound)	Traveling direction, right	1
New observation	July 5, 2017 Around 12:11						

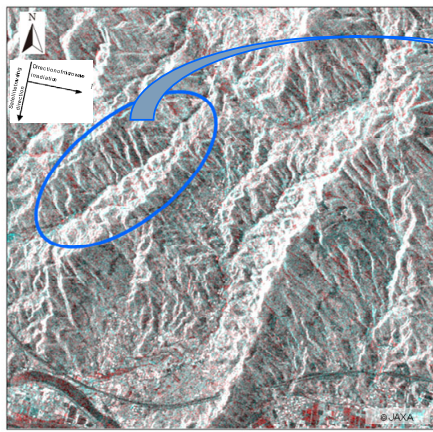
Northern Kyushu Torrential Rainfall in July 2017

■ Conditions of/time required for image interpretation survey

Disaster factor	Date & time of disaster occurrence	Meteorological situation during disaster occurrence	Image interpretation area [km ²]	[A] Disaster occurrence - SAR observation	[B] SAR observation - Image interpretation survey	[A+B] Disaster occurrence - Image interpretation survey
Rainfall	2017/7/5 14:10	Rainy Clear from the morning, next day	About 3,500	46hours42minutes	7hours08minutes	53hours50minutes

■ Image interpretation survey timeline

Date & time	Transmitter	Receiver	Response, etc.
2017/7/5 14:10	-	-	Sediment disaster warning information was announced in Asakura City and Toho Village, Fukuoka Prefecture.
2017/7/5 17:51	-	-	Special heavy rain warning was announced in Fukuoka Prefecture.
Around 20:00	MLIT Headquarters	JAXA	ALOS-2 Emergency Observation Request
Starting at around 6:00 on July 6, the Regional Development Bureau started helicopter survey after waiting for the weather to get better. => Frequent occurrences of sediment disasters were identified in Asakura City.			
Around 2017/7/7 12:52	-	-	ALOS-2 observation
14:16	JAXA	NILIM	ALOS-2 observation data was provided; started image interpretation
17:21	NILIM	MLIT Headquarters	Reported the results of image interpretation (quick report) in the major places hit by the disaster that were reported in news media.
18:01	NILIM	MLIT Headquarters	Reported the results of image interpretation in major extracted places on the north side of Toho Village.
Around 20:00	NILIM	MLIT Headquarters	Reported the results of image interpretation (the entire image interpretation range). Provided information to the Kyushu Regional Development Bureau.



(Left) Intensity difference SAR image around Asakura City



(Right) Area where failure occurred frequently that was identified by the

■ Parameters of the SAR images used for the image interpretation survey

	Observation date & time	Resolution [m]	Off nadir angle [°]	Polarization	Orbit direction	Direction of microwave irradiation	Number of scenes
Archive	April 29, 2016 Around 12:52	3	29.1 (U2-6)	HH	Descending (Southbound)	Traveling direction, left	1
New observation	July 7, 2017 Around 12:52						

2017 Typhoon No. 21

■ Conditions of/time required for image interpretation survey

Disaster factor	Date & time of disaster occurrence	Meteorological situation during disaster occurrence	Image interpretation area [km ²]	[A] Disaster occurrence - SAR observation	[B] SAR observation - Image interpretation survey	[A+B] Disaster occurrence - Image interpretation survey
Rainfall	2017/10/22 16:00	Rainy	About 6,000	19hours29minutes	7hours20minutes	26hours49minutes

■ Image interpretation survey timeline

Date & time	Transmitter	Receiver	Response, etc.
2017/10/22 16:00	-	-	Sediment disaster warning information was announced in Shingu City, Wakayama Prefecture, and others.
2017/10/23 09:33	Kinki Regional Development Bureau	MLIT Headquarters	Request for SAR image observation
Around 11:29	-	-	ALOS-2 observation
14:04	JAXA	NILIM	ALOS-2 observation data was provided; started image interpretation.
18:35	JAXA	MLIT Headquarters - NILIM	Reported the results of image interpretation.
18:49	NILIM	MLIT Headquarters	Reported the findings in the results of image interpretation.

■ Parameters of the SAR images used for the image interpretation survey

	Observation date & time	Resolution [m]	Off nadir angle [°]	Polarization	Orbit direction	Direction of microwave irradiation	Number of scenes
New observation	October 23, 2017 Around 11:29	6	56.2 (U5-21)	HV	Descending (Southbound)	Traveling direction, left	3

2018 Northern Osaka Earthquake

■ Conditions of/time required for image interpretation survey

Disaster factor	Date & time of disaster occurrence	Meteorological situation during disaster occurrence	Image interpretation area [km ²]	[A] Disaster occurrence - SAR observation	[B] SAR observation - Image interpretation survey	[A+B] Disaster occurrence - Image interpretation survey
Earthquake	2018/6/18 07:58	Cloudy - Rainy Bad weather conditions continued until around 21st.	About 3,500	16hours00minutes	9hours10minutes	25hours10minutes

■ Image interpretation survey timeline

Date & time	Transmitter	Receiver	Response, etc.
2018/6/18 07:58	-	-	An earthquake occurred in the northern part of Osaka Prefecture (a maximum seismic intensity of 6 lower was observed in Kita Ward, Osaka City, Takatsuki City, Hirakata City, Ibaraki City, and Minoh City).
08:34	MLIT Headquarters	JAXA	ALOS-2 Emergency Observation Request
Around 23:58	-	-	ALOS-2 observation
2018/6/19 Around 01:00	JAXA	NILIM	ALOS-2 observation data was provided.
Around 07:00	NILIM	-	Started image interpretation.
08:06	JAXA	NILIM	Sent the results of image interpretation.
09:08	NILIM	MLIT Headquarters	Reported the findings in the results of image interpretation.
Starting at around 9:30 on June 19, the Regional Development Bureau started helicopter survey. => No major damage was identified.			

■ Parameters of the SAR images used for the image interpretation survey

	Observation date & time	Resolution [m]	Off nadir angle [°]	Polarization	Orbit direction	Direction of microwave irradiation	Number of scenes
Archive	April 9, 2018 Around 23:58	3	38.2 (U2-9)	HH	Ascending (Northbound)	Traveling direction, right	1
New observation	June 18, 2018 Around 23:58						

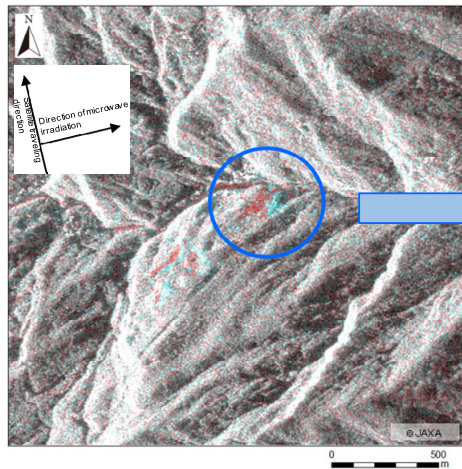
Torrential Rainfall in July 2018

■ Conditions of/time required for image interpretation survey

Disaster factor	Date & time of disaster occurrence	Meteorological situation during disaster occurrence	Image interpretation area [km ²]	[A] Disaster occurrence - SAR observation	[B] SAR observation - Image interpretation survey	[A+B] Disaster occurrence - Image interpretation survey
Rainfall	2018/07/06 14:10	Rainy	About 10,000	33hours54minutes	7hours56minutes	41hours50minutes

■ Image interpretation survey timeline

Date & time	Transmitter	Receiver	Response, etc.
2018/07/06 14:05	-	-	Sediment disaster warning information was announced in Hiroshima City, Hiroshima Prefecture, and others. A
Around 17:00	MLIT Headquarters	JAXA	ALOS-2 Emergency Observation Request
19:40	-	-	Special heavy rain warning was announced in Hiroshima, Okayama, and Tottori Prefectures.
2018/07/08 Around 00:04	-	-	ALOS-2 observation B
Around 03:50	JAXA	NILIM	ALOS-2 observation data was provided; started image interpretation.
Around 08:00	NILIM	Chugoku/Shikoku Regional Development Bureaus	Reported the results of image interpretation.



(Left) Place of sediment movement reported during SAR image interpretation



(Right) Large-scale failure identified at the site

■ Parameters of the SAR images used for the image interpretation survey

	Observation date & time	Resolution [m]	Off nadir angle [°]	Polarization	Orbit direction	Direction of microwave irradiation	Number of scenes
Archive	April 14, 2018 Around 00:04	3	38.2 (U2-9)	HH	Ascending (Northbound)	Traveling direction, right	4
New observation	July 8, 2018 Around 00:04						

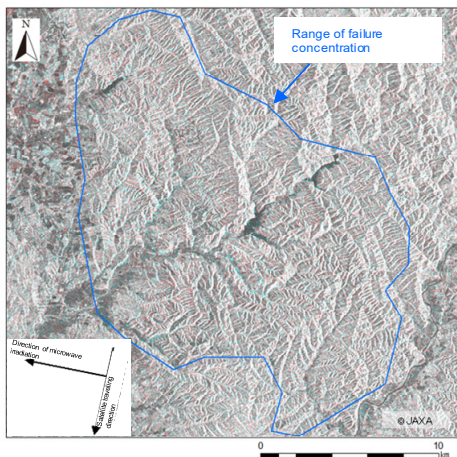
2018 Hokkaido Eastern Iburi Earthquake

■ Conditions of/time required for image interpretation survey

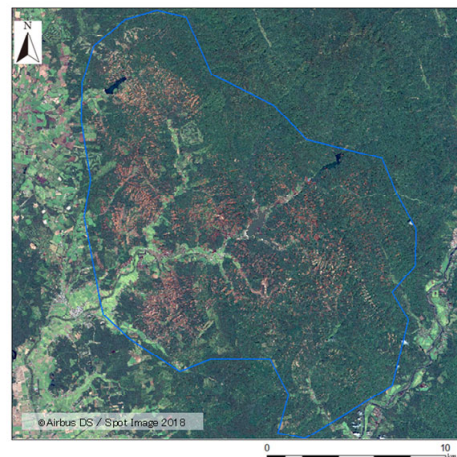
Disaster factor	Date & time of disaster occurrence	Meteorological situation during disaster occurrence	Image interpretation area [km ²]	[A] Disaster occurrence - SAR observation	[B] SAR observation - Image interpretation survey	[A+B] Disaster occurrence - Image interpretation survey
Earthquake	2018/9/6 03:07	Cloudy - Rainy Bad weather conditions continued for a while after occurrence of the disaster.	About 3,000	8hours34minutes	3hours49minutes	12hours23minutes

■ Image interpretation survey timeline

Date & time	Transmitter	Receiver	Response, etc.
2018/9/6 03:07	-	-	Occurrence of the disaster
Around 04:00	MLIT Headquarters	JAXA	ALOS-2 Emergency Observation Request
Around 11:41	-	-	ALOS-2 observation
Around 14:12	JAXA	NILIM	ALOS-2 observation data was provided; started image interpretation.
Starting at around 15:00, the Regional Development Bureau started helicopter survey after waiting for the weather to get better.			
Around 15:30	NILIM	Hokkaido Regional Development Bureau	Provided the results of image interpretation. Reported the range where slope failures concentrate estimated by SAR images speedily.
Much time was required to grasp the situation of damage by means of optical images due to bad weather conditions.			
2018/9/11 Around 09:42	-	-	Observation by means of optical satellites Confirmed that the range of failure concentration roughly coincides with the range obtained by image interpretation of SAR images.



(Left) Range of failure concentration reported during image interpretation of SAR images



(Right) Range of failure concentration confirmed by optical satellites

■ Parameters of the SAR images used for the image interpretation survey

	Observation date & time	Resolution [m]	Off nadir angle [°]	Polarization	Orbit direction	Direction of microwave irradiation	Number of scenes
Archive	August 23, 2018 Around 11:41	3	32.4 (U2-7)	HH	Descending (Southbound)	Traveling direction, right	2
New observation	September 6, 2018 Around 11:41						

2017 Torrential Rain in southwestern Sri Lanka

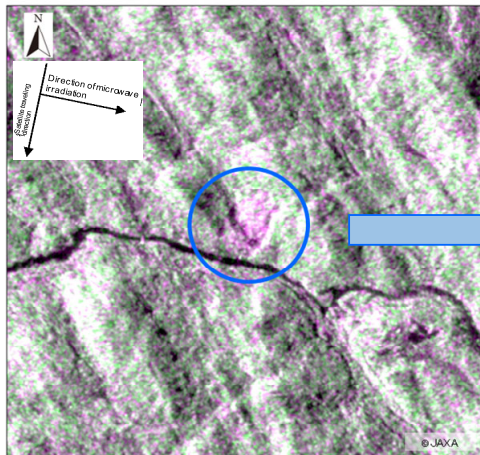
■ Conditions of/time required for image interpretation survey

Disaster factor	Date & time of disaster occurrence	Meteorological situation during disaster occurrence	Image interpretation area [km ²]	[A] Disaster occurrence - SAR observation	[B] SAR observation - Image interpretation survey	[A+B] Disaster occurrence - Image interpretation survey
Rainfall	2017/5/24~26	Rainy	About 5,600	144hours00minutes	29hours00minutes	173hours00minutes

■ Image interpretation survey timeline

Date & time	Transmitter	Receiver	Response, etc.
2017/5/24~26	-	-	Sediment disasters occurred in southwestern Sri Lanka due to record-breaking torrential rainfalls.
2017/5/29	MLIT Headquarters	JAXA	ALOS-2 Emergency Observation Request
2017/5/30	-	-	ALOS-2 observation
2017/5/31 Around 08:30	JAXA	NILIM	ALOS-2 observation data was provided; started image interpretation
17:00	NILIM	MLIT Headquarters	Reported the findings in the results of image interpretation.
2017/6/1	NILIM	JICA	Provided the results of image interpretation.

June 6 The Japan Disaster Relief Team conducted site survey based on the results of image interpretation. => Confirmed a large-scale failure.



(Left) Place where sediment movement occurred reported during the image interpretation of SAR images

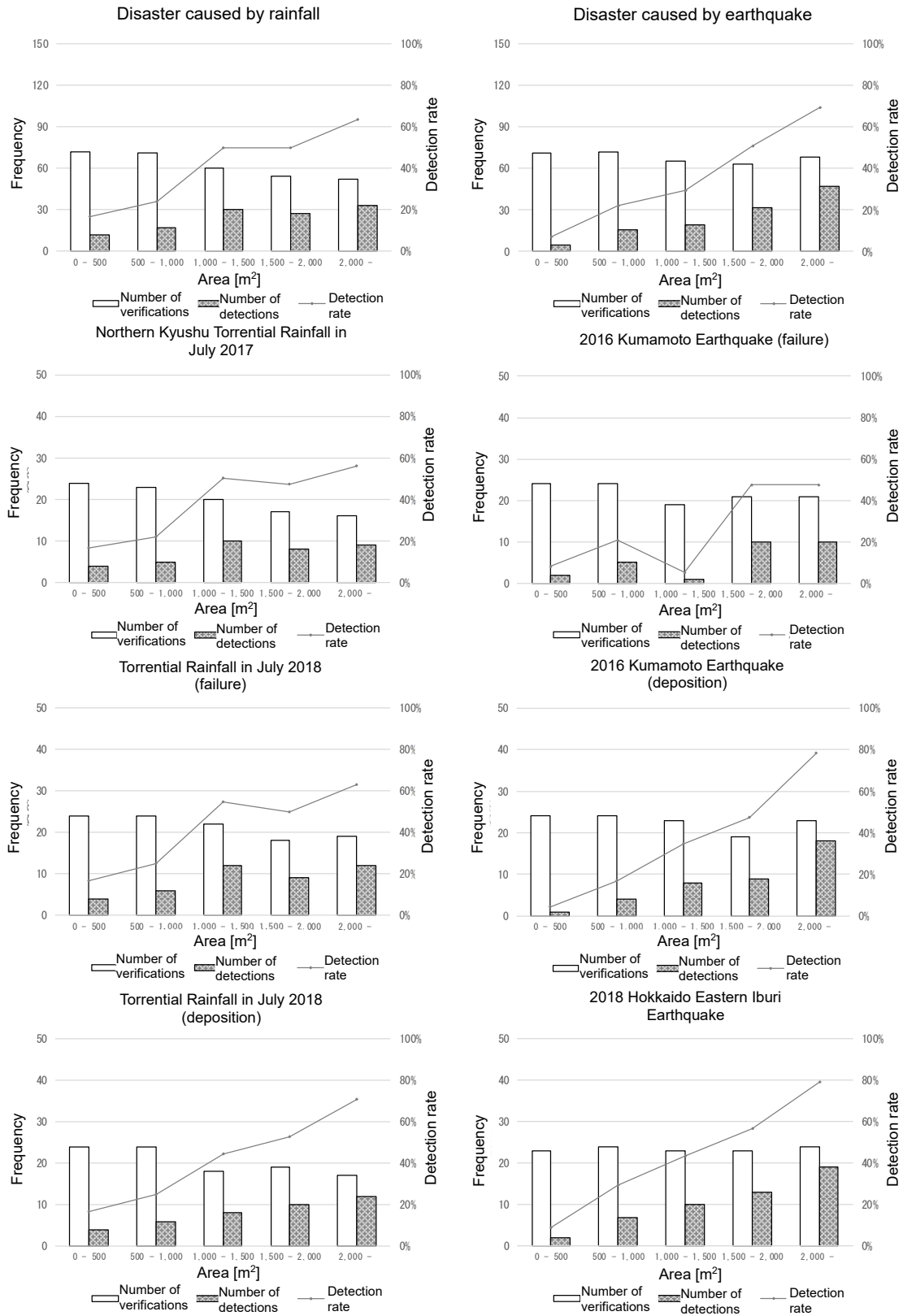


(Right) Large-scale failure confirmed at the site.

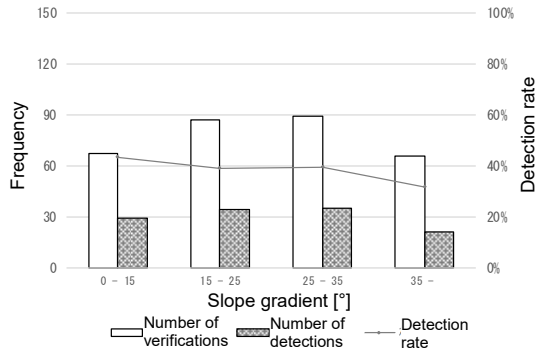
■ Parameters of the SAR images used for the image interpretation survey

	Observation date & time	Resolution [m]	Off nadir angle [°]	Polarization	Orbit direction	Direction of microwave irradiation	Number of scenes
New observation	2017/10/23 Daytime path	10	39.3	HV	Descending (Southbound)	Traveling direction, left	3

Reference material 2. Accuracy of the image interpretation survey of sediment disasters by means of intensity difference SAR images in each disaster

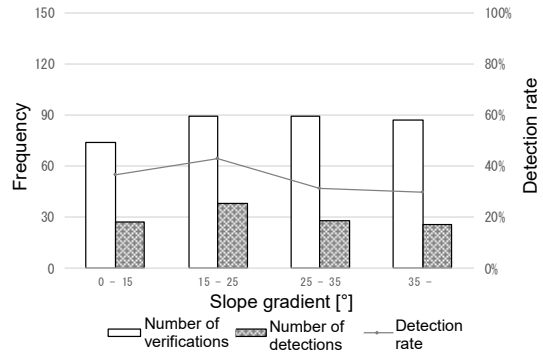


Disaster caused by rainfall

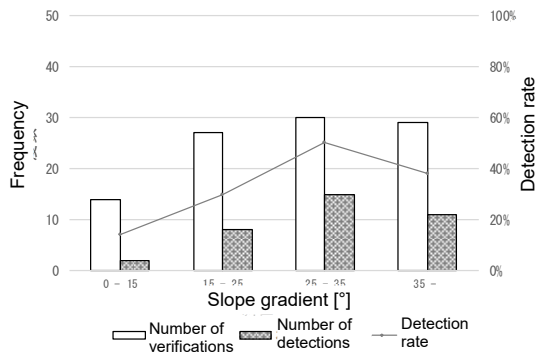


Northern Kyushu Torrential Rainfall in July 2017

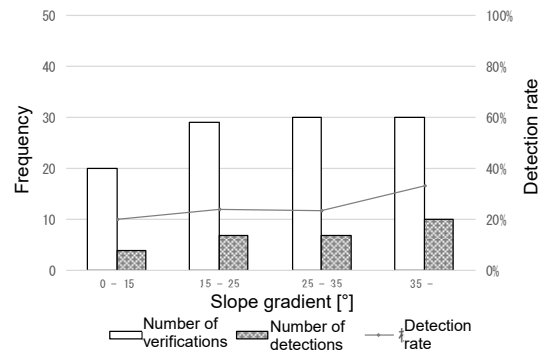
Disaster caused by earthquake



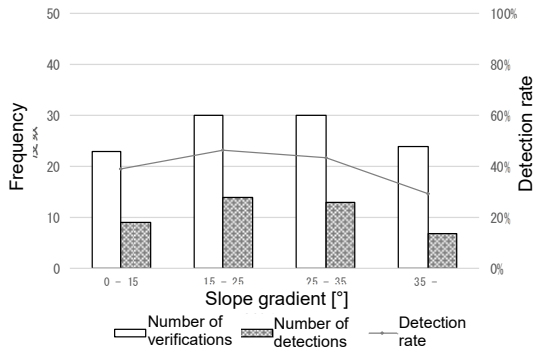
2016 Kumamoto Earthquake (failure)



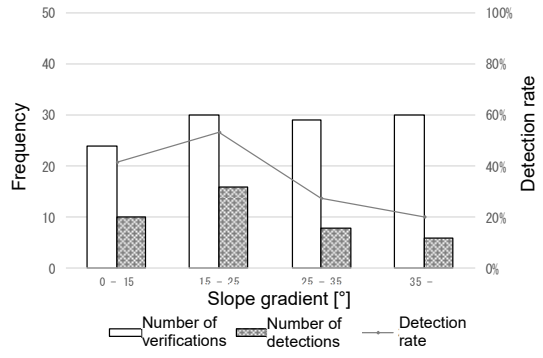
Torrential Rainfall in July 2018 (failure)



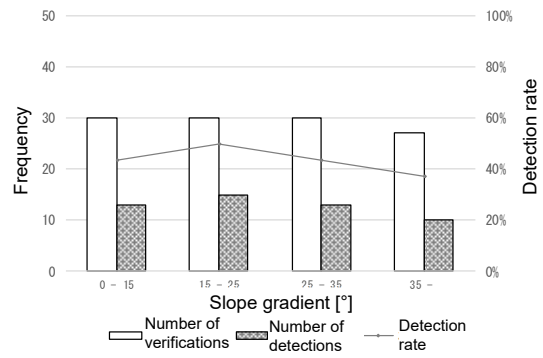
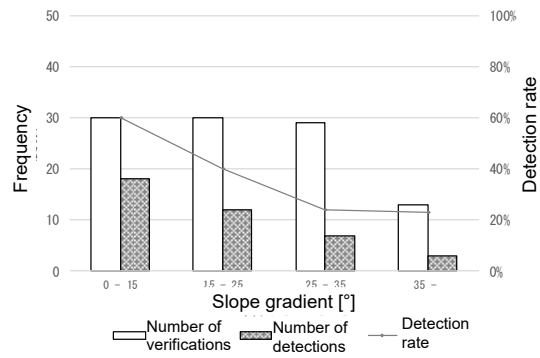
2016 Kumamoto Earthquake (deposition)

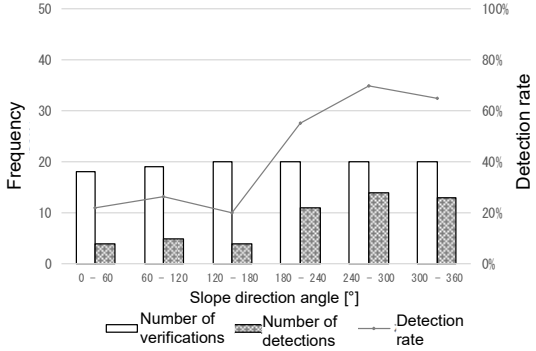
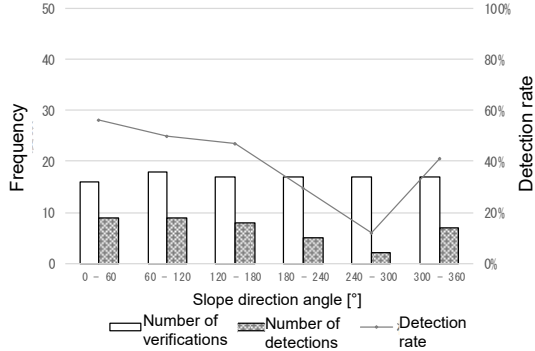
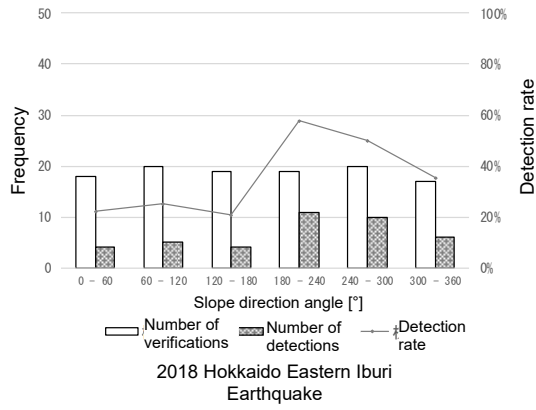
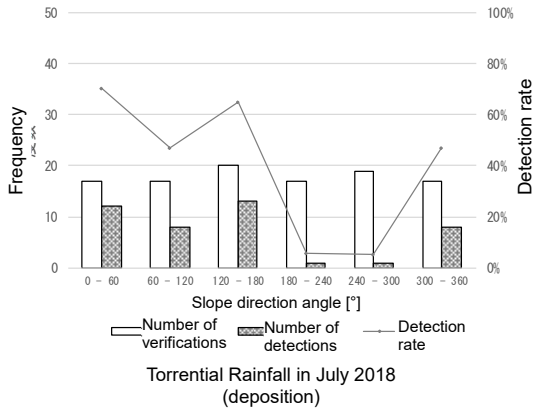
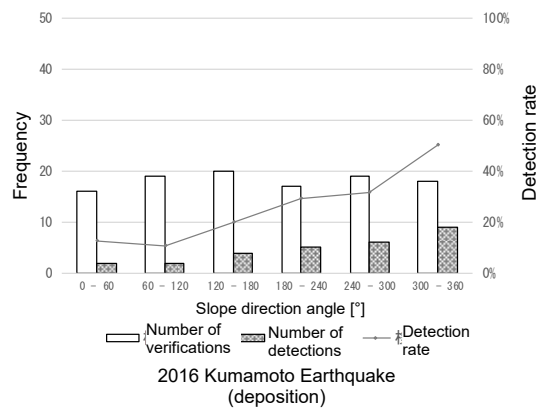
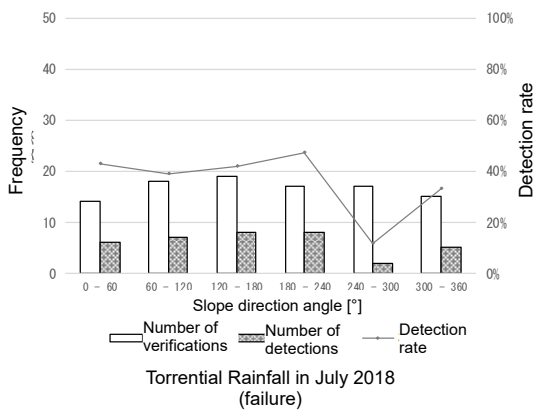
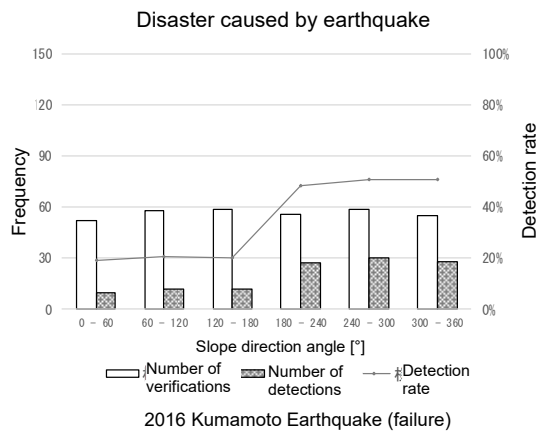
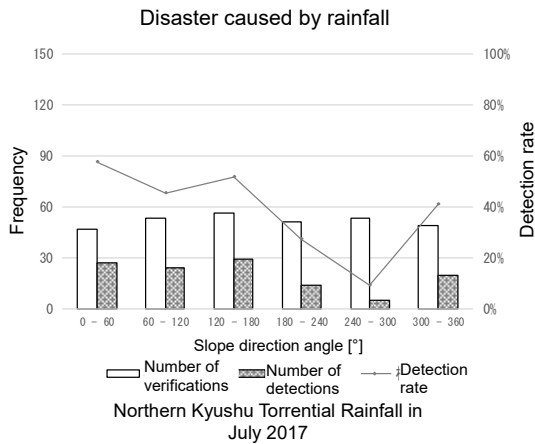


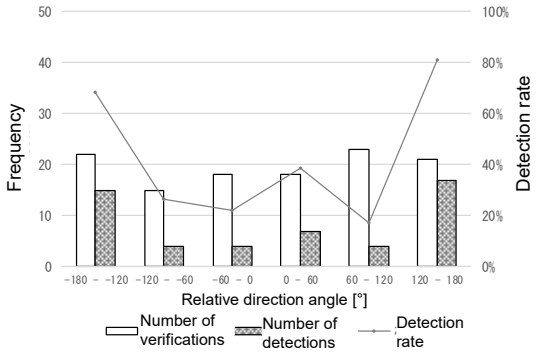
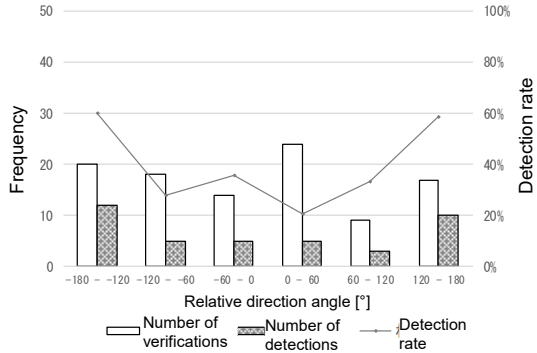
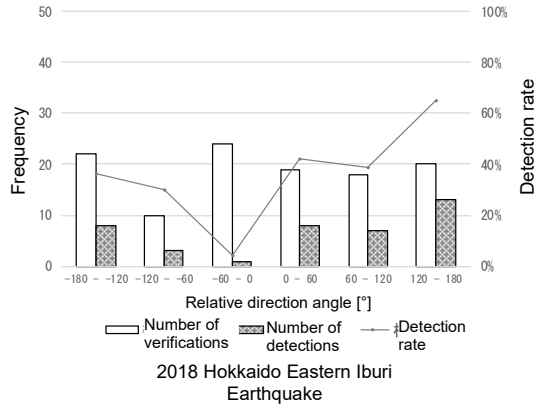
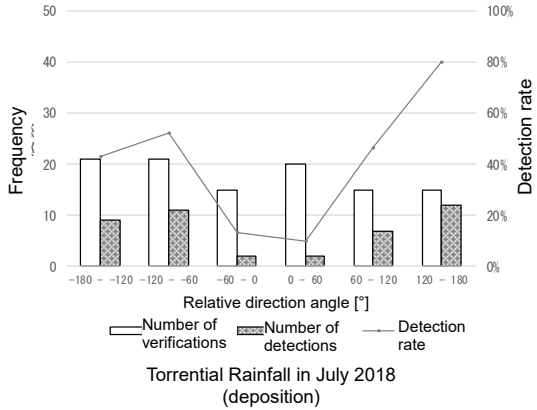
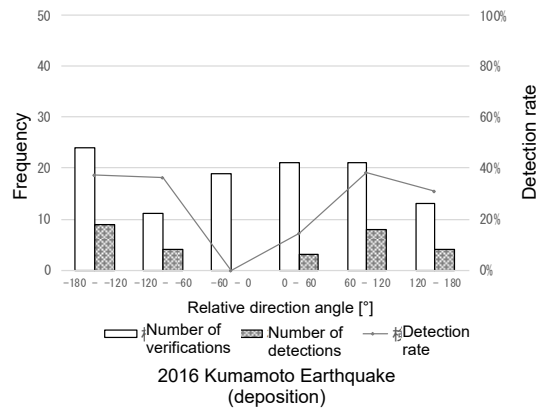
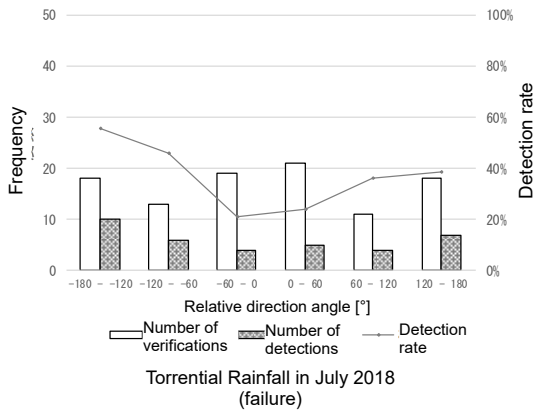
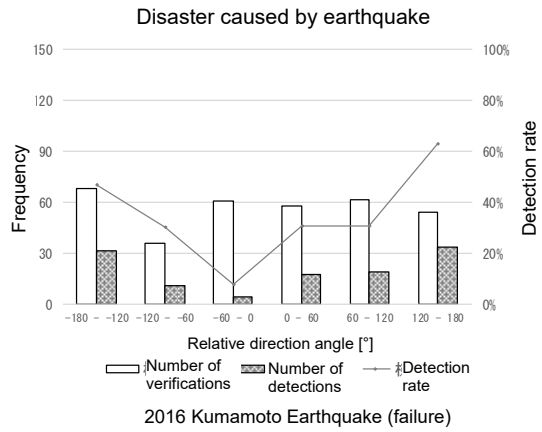
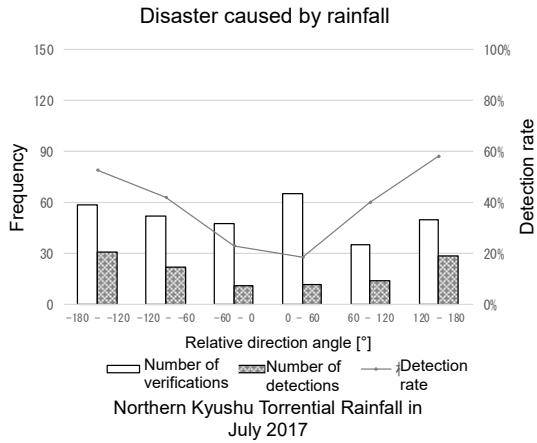
Torrential Rainfall in July 2018 (deposition)

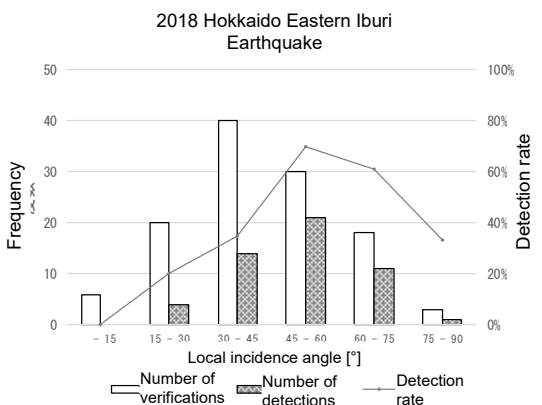
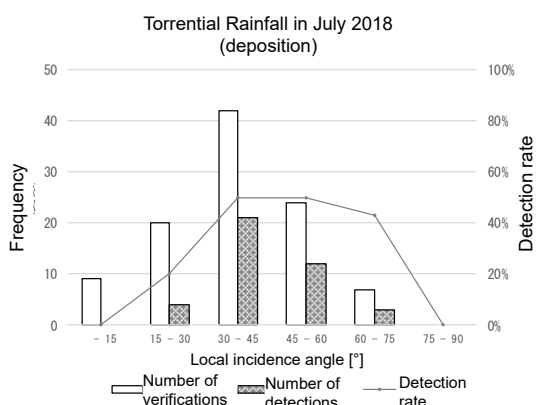
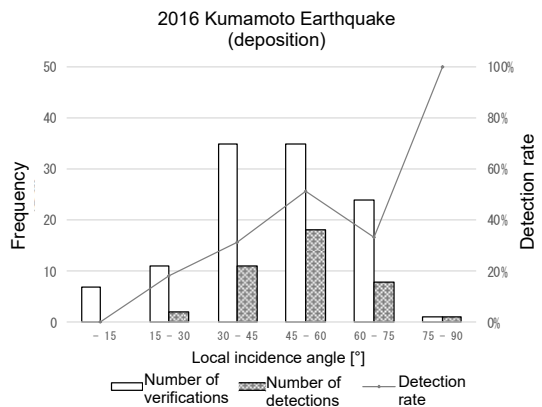
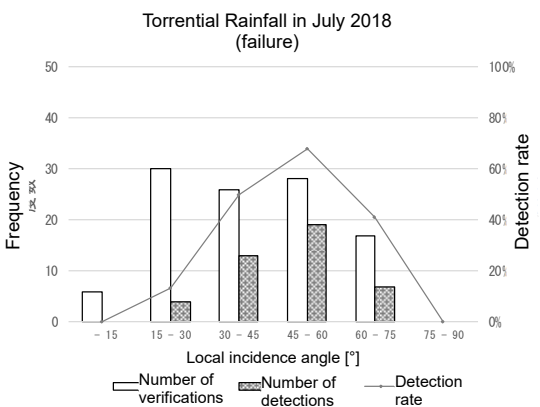
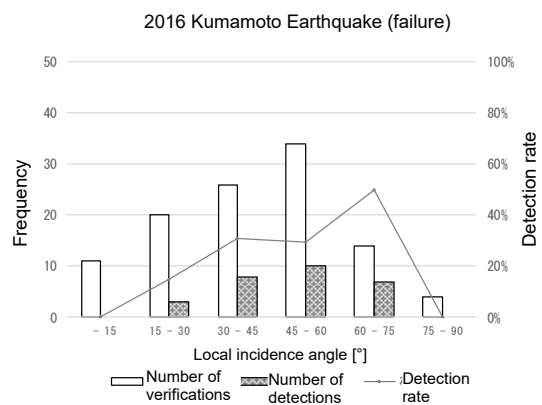
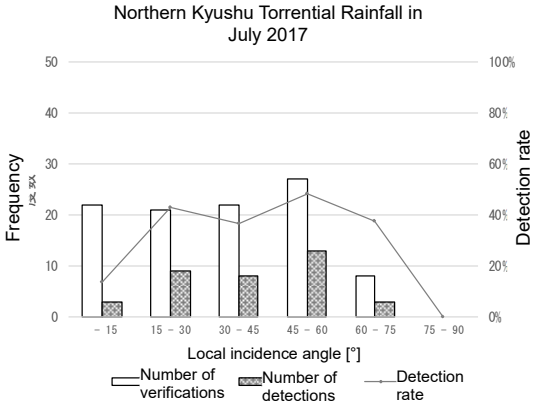
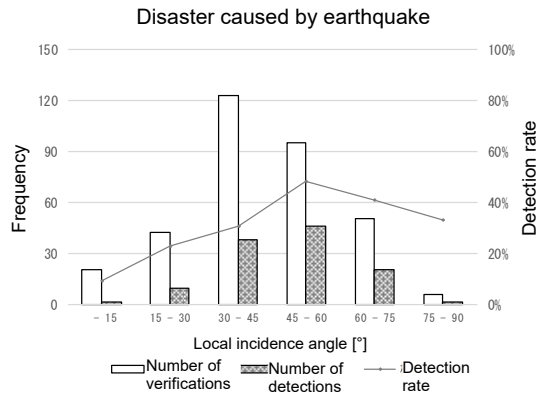
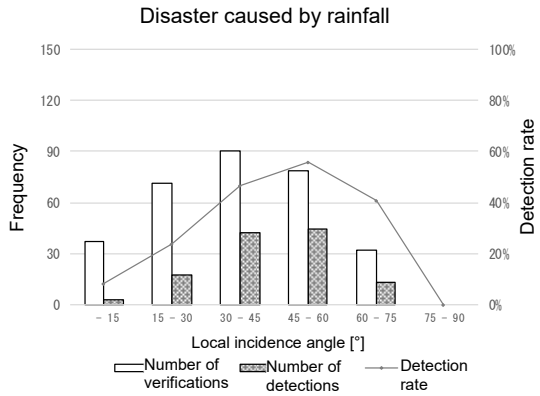


2018 Hokkaido Eastern Iburi Earthquake









Reference material 3. Checklist of the image interpretation survey of sediment disasters by means of intensity difference SAR images

Intensity difference SAR image	Single-polarized SAR image (before disaster)	Single-polarized SAR image (after disaster)
Topographical map	Optical image before disaster	

Step	Images, etc. to be referred to	Range to be checked	Check item	Judgment criteria	Evaluation (O×)
1	Intensity difference SAR image	Coloring range of intensity difference SAR image	Dominant color	(1) Red or red/cyan pairs can be seen	
				(2) Cyan can be seen	
	Single-polarized SAR image	Changes in single-polarized SAR image before and after the disaster	Shape change	(3) Appears to be dented (4) Appears to have swollen	
	Intensity difference SAR image	Coloring range of intensity difference SAR image	Clarity	(5) Is clear	

(1),(3): O => 2 (failure) (2), (4): O => 2 (deposition)

2 (failure)	Topographical map	Topography	Slope gradient	(6) Is an inclined land	
	Topographical map Optical image before disaster	Surroundings	Land cover	(7) Not an artificially modified land	
	Topographical map Optical image before disaster	Surroundings	Land cover	(8) Is a forest	
2 (deposition)	Topographical map	Topography	Slope gradient	(9) Is a flat land	
	Topographical map Optical image before disaster	Surroundings	Land cover	(10) Not an artificially modified land	
	Topographical map Optical image before disaster	Surroundings	Positional relationship	(11) Is adjacent to changes in red	

3	Intensity difference SAR image	In the channel	Dominant color	(12) Cyan can be seen	
		Upstream side of the channel		(13) Red can be seen	
	Topographical map Optical image before disaster	Upstream side of the channel	Inundated facility	(14) No inundated facility	

Judgment results	<p>a. Occurrence of a slope failure May have occurred / Changes cannot be verified</p> <p>b. Sediment deposition caused by a failure May have occurred / Changes cannot be verified</p> <p>c. Formation of channel blockage May have occurred / Changes cannot be verified</p> <p>d. Image interpretation cannot be made sufficiently from SAR images</p>
-------------------------	--

.....
TECHNICAL NOTE of NILIM

No.1110 April 2020

© National Institute for Land and Infrastructure Management

.....
National Institute for Land and Infrastructure Management

Ministry of Land, Infrastructure, Transport and Tourism

1, Asahi, Tsukuba, Ibaraki, 305-0804 Japan

Phone:+81-(0)29-864-2675